Wind Energ. Sci. Discuss., doi:10.5194/wes-2016-43, 2016
Manuscript under review for journal Wind Energ. Sci.
Published: 1 December 2016

eawe european academy of wind energy
Open Access WIND ENERGY SCIENCE DISCUSSIONS

An intercomparison of mesoscale models at simple sites for wind energy applications

Bjarke Tobias Olsen, Andrea N. Hahmann, Anna Maria Sempreviva, Jake Badger, and Hans E. Jørgensen
DTU Wind Energy, Frederiksborgvej 399, 4000 Roskilde, Denmark
Correspondence to: Bjarke Tobias Olsen (btol@dtu.dk)

Abstract. An intercomparison of model results from 25 different Numerical Weather Prediction (NWP) models is presented for the year 2011 at six sites in Northern Europe characterized by simple terrain. The model results and a detailed description of each model was submitted by 18 different modeling groups to a open call for data, and serves as a rare quantitative overview of the model uncertainties associated with state-of-the-art mesoscale models used for wind energy applications today. At three of the sites the model intercomparison was verified with observations from nearby meteorological masts. The intercomparison was based on statistical properties of the wind for a number of heights at each site.

The results show better performance of the models and a smaller inter-model spread offshore and aloft ($2-4\%$ mean wind speed bias above 40 meters), and greater errors and more spread for inland sites and closer to the surface (up to $7-9\%$ wind speed bias). For the distributions of wind speed, wind direction, and wind shear only small deviations exist between the observations and the average of the models, but a small shift of the average wind speed distribution towards high wind speeds at Cabauw, and an underrepresentation of strong shear cases was observed. Although the model setup options were studied to determine a 'best practice', no significant indicator was found.

1 Introduction

Numerical Weather Prediction (NWP) models are increasingly being used for wind energy related applications, ranging from site assessment, development and planning of wind farms, to power-forecasting, maintenance, and energy trading on the electricity markets. For site assessment, NWP models are commonly part of the model chain used for estimation of the Annual Energy Production (AEP). However, a large part of the uncertainty in the estimate is contributed by the uncertainties of the NWP model. This, combined with the extensive use of these models, and the fact that each model typically has multiple options and parameters available for each sub-component, means that a strong demand exists for quantification of a) the sensitivity to the choice of sub-components and parameters, and b) the overall model uncertainties. Having a better understanding of the sensitivities and uncertainties of NWP models can help lower the associated risks, and improve decision making, which in turn will lower the Levelized Cost of Energy (LCOE). For model users, having access to sensitivity quantification of individual model components enables optimization of the model setup for specific applications. In the following, the NWP models in the study will sometimes be referred to as 'mesoscale' models, signifying that they partly resolve weather phenomena in

Wind Energ. Sci. Discuss., doi:10.5194/wes-2016-43, 2016
Manuscript under review for journal Wind Energ. Sci.
Published: 1 December 2016

eawe european academy of wind energy
Open Access WIND ENERGY SCIENCE DISCUSSIONS

the mesoscale range, defined as horizontal length scales from about one kilometer, up to several hundreds of kilometers, i.e. (Orlanski, 1975).

A common way to assess NWP model uncertainties is to use an ensemble approach, where a number of parallel model runs, referred to as a ensemble members, are run with slightly perturbed initial conditions for each ensemble member, see e.g. Warner (2004) for details. The magnitude of the perturbations are typically limited by the uncertainty associated with the particular perturbed variable, in the hope that the ensemble of solutions will cover the solution-space arising from the uncertainties of the input parameters. Ensemble-based techniques are used for many meteorological application, including: precipitation forecasting (Gebhardt et al., 2011; Bowler et al., 2006), wind power generation forecasting (Constantinescu et al., 2011), and resource assessment (Al-Yahyai et al., 2012). However, one would not expect that the ensembles of one particular modeling system fully represent the uncertainties of another modeling system. This was shown in the DEMETER project (Development of a European Multimodel Ensemble for seasonal to inTERannual climate prediction) (Palmer et al., 2004), which also demonstrated that a multimodel ensemble approach consisting of a number of different modeling systems, each split into a number of ensembles, does a much better job at representing the overall uncertainties than any single model ensemble.

NWP model sensitivities related to individual model components have been studied in great detail in the last couple of decades, in many different climates and terrains. In Northern Europe the sensitivities of the Weather Research and Forecasting (WRF) model (Skamarock et al., 2008a) have been studied for coastal and offshore locations in several recent papers: Vincent and Hahmann (2015) studied the effect of grid nudging, spin-up, and simulation time, on near-surface and upper PBL wind speed variance for the model in the North Sea and the Baltic Sea. One 'short' setup with 36 hours simulation time, including 12 hours of spin-up, and no grid nudging, was compared to two 'long' simulations of 11 days, with a one day spin-up, one using grid nudging above the Planetary Boundary Layer (PBL), and one using spectral nudging. The study showed that while spatial smoothing is observed when nudging is used, it has little impact in the lower part of the atmosphere, and it is concluded that the setups using longer simulation time are appropriate for wind energy applications. Draxl et al. (2014) ran the WRF model at a coastal site in Denmark with seven different PBL schemes, in order to study how well the model represents profiles of wind speed and wind shear at heights from 10 to 160 meters, using the different schemes. The study shows that the Yonsei University (YSU) (Hong et al., 2006) PBL scheme represented the wind climate best for unstable atmospheric stability conditions, while the Asymmetric Convective Model version 2 (ACM2) (Pleim, 2007b), and the Meller-Yamada-Janjic (MYJ) (Janjić, 1994) PBL schemes worked better for neutral and stable conditions respectively. In Hahmann et al. (2014b) the WRF model sensitivities over the Baltic and North Seas were studied for the following model components: the dataset used for initial and boundary condition, the PBL scheme, the number of vertical grid levels, and the source of Sea Surface Temperature (SST) data. A year long wind climatology simulation was used as the test variable. The study showed that the choice of PBL scheme and spin-up time had the strongest impact on the observed mean wind speed, while the other components played a lesser role.

The WRF model sensitivities have also been studied in regions of complex terrain. Carvalho et al. (2012) studied the sensitivities to the choice of restart frequency, grid nudging, and suite of Surface Layer (SL) scheme, PBL scheme, and Land Surface Model. They observe that using grid nudging and frequent restarts (every 2 days) gives the best agreement with several masts

Wind Energ. Sci. Discuss., doi:10.5194/wes-2016-43, 2016
Manuscript under review for journal Wind Energ. Sci.
Published: 1 December 2016

eawe european academy of wind energy
Open Access WIND ENERGY SCIENCE DISCUSSIONS

located in complex terrain, and that a seasonal dependency of the optimal suite of SL-PBL-LSM exists. A seasonal dependency was found by García-Díez et al. (2013) who looked at systematic biases for the year 2011 for all of Europe, by comparing gridded observations, upper-air data, and high-frequency station observations, with three WRF runs using different PBL schemes. They also warn that sensitivity studies based on a limited period may not be representative for the whole year. In Carvalho et al. (2014b) the sensitivities to the choice of SL and PBL scheme is also studied by comparing the model runs to 13 land-based masts and five offshore buoys. The study shows that the PX SL scheme (Pleim, 2006) and ACM2 PBL scheme (Pleim, 2007b) gave the smallest errors for wind energy related metrics. However, for offshore only sites the smallest errors were given by the model using the QNSE-QNSE PBL scheme and SL scheme (Sukoriansky et al., 2005). A similar study by Gómez-Navarro et al. (2015) analysed the sensitivities the WRF model to the choice of PBL scheme, grid spacing and setup in complex terrain in Switzerland. The evaluation metric was the near surface wind at a number of masts all over the country. The study showed, for their suite of setups, that using the YSU PBL scheme, the highest spacial resolution (2 km), and Analysis Nudging, gave the best agreements with measurements during a number of wind storms. Carvalho et al. (2014a) studied the sensitivities to the choice of dataset for initial and boundary conditions, and showed that using the ECMWF (European Center for Medium-range Weather Forecast) ERA-Interim reanalysis dataset (Simmons et al., 2007) gave the best agreement with wind measurements at several sites of high wind resource, when compared to the NCEP (National Centers for Environmental Prediction) R2 (Kanamitsu et al., 2002), CFSR (Saha et al., 2010), FNL, and GFS datasets, as well as the NASA (National National Aeronautics and Space Administration) MERRA dataset (Rienecker et al., 2011). Schicker et al. (2016) studied the temperature sensitivities to the choice of land use dataset in two regions in Austria characterized by complex terrain, such sensitivites can be relevant for wind energy if they influence the wind by misrepresenting the atmospheric stability characteristics. Their study showed that, in general, when compared to surface, upper air, and satellite observations of temperature and wind speed, the CORINE CLC06 dataset (Büttner et al., 2004) gave better model agreements than the USGS (Garbarino et al., 2002), and MODIS (Friedl et al., 2010) datasets.

Several intercomparison studies of NWP models for near-surface wind and resource assessment exists. In Horvath et al. (2012) the MM5 (Grell et al., 1994) and WRF models were compared for a site in west-central Nevada characterized by complex terrain. Both models were run in a grid nesting setup from 27 kilometers to 333 meters, and the near-surface wind were compared to wind observations from several 50 meter tall towers. The study showed that WRF model gave better agreement with mean wind speed observations, but it suffered from an overestimation of intensity and frequency of thermally driven flow. In Hahmann et al. (2015) two downscaling methodologies: KAMM-WAsP (Badger et al., 2014) and WRF Wind Atlas (Hahmann et al., 2014a), both based on a coupling approach between a NWP model and a simple microscale model using a linearized flow model, were intercompared for a number of mast sites in South Africa. The study showed that the WRF-based method gave smaller biases than the KAMM-based approach, which were shown to underestimated the wind speeds.

So, while extensive work has been put in assessing model sensitivities to initial initial conditions, by e.g. many-model ensemble studies, and into studying the sensitivities to choice of model components, by e.g. case-control studies, little knowledge has been derived from assessing the operational NWP models run by the community. However, in the last decade, several intercomparison studies have been succesfully carried out for other types of models based on model output submitted by modelers from

Wind Energ. Sci. Discuss., doi:10.5194/wes-2016-43, 2016
Manuscript under review for journal Wind Energ. Sci.
Published: 1 December 2016

the wind energy community, including the Bolund experiment and the CREYAP exercise. The Bolund experiment (Bechmann et al., 2011) was an intercomparison of flow models, from simple models to Computational Fluid Dynamics (CFD) models. The modelers were asked to model the flow around the small island of Bolund in Denmark, and the model results were verified using observations from a previous measurement campaign (Berg et al., 2011). The Comparison of Resource and Energy Yield Assessment Procedures (CREYAP) (Mortensen et al., 2015) was an intercomparison study of energy yield assessment procedures based on four case-studies. The study revealed a large spread among the different procedures, and highlighted the need for further studies into the uncertainties associated with the models. Carrying out a similar type of intercomparison study for NWP models can be attractive for a number of reasons, including: 1) It offers an opportunity, not just for model developers to get a better understanding of the model uncertainties, but also for users and stake-holders in the wind energy community whom rely on these models. 2) It reduces the workload required to carry out comparative studies because the data, in most cases, already exists, and it increases scalability because including additional model results require very little effort compared to traditional studies. 3) Depending on the level of meta-data collected, it offers a unique insight into what the community considers 'best-practice' when it comes to NWP modeling for wind energy applications.

In the present study a blind intercomparison of 25 different NWP models is presented for six simple sites in northern Europe. It is co-organized by the European Wind Energy Association (EWEA) and the European Energy Research Alliance Joint Programme Wind Energy (EERA JP WIND), and based on model output submitted from the modeling community to an open call for data. The six sites represent some of the simplest terrain for the models. They are all located offshore or in mostly flat and homogeneous terrain, where the subgrid-scale parameterizations of the models are expected to work well. Three sites have a tall meteorological mast with observations at many heights available for verification of the model results. The two main aims of the study are: 1) To highlight and quantify the uncertainties of the models, and to serve as motivation and indicator for future analysis of model uncertainties. 2) To identify model setup decisions that have an impact on model performance. The models are intercompared using simple metrics relevant for wind energy applications.

The structure of the paper is as follows: In sect. 2 a detailed description of the methodology used in this study is presented, including a description of the six study sites and the models used by the participants. In sect. 3 the intercomparison results are shown. A discussion of the results is given in sect. 4, and finally in sect. 5 the conclusions of the study are presented.

2 Methodology

2.1 Mast sites and observations

The six locations chosen for the intercomparison are labeled FINO3, Høvsøre, Cabauw, and Dataless1-3, is shown in Fig 1, and the location and type of the sites are shown in Table A1. Three of the sites correspond to the locations of tall meteorological masts, located in terrain of different characteristics: land, coastal, and offshore. The mast sites have long-term records of observations and serve as the main intercomparison sites. The year 2011 was selected as the case-study due to excellent availability of observations. The three observation-less sites were selected because they each resemble one of the mast-sites, and serve to identify whether a consistent pattern of intermodel variance exists between similar sites.

Wind Energ. Sci. Discuss., doi:10.5194/wes-2016-43, 2016
Manuscript under review for journal Wind Energ. Sci.
Published: 1 December 2016

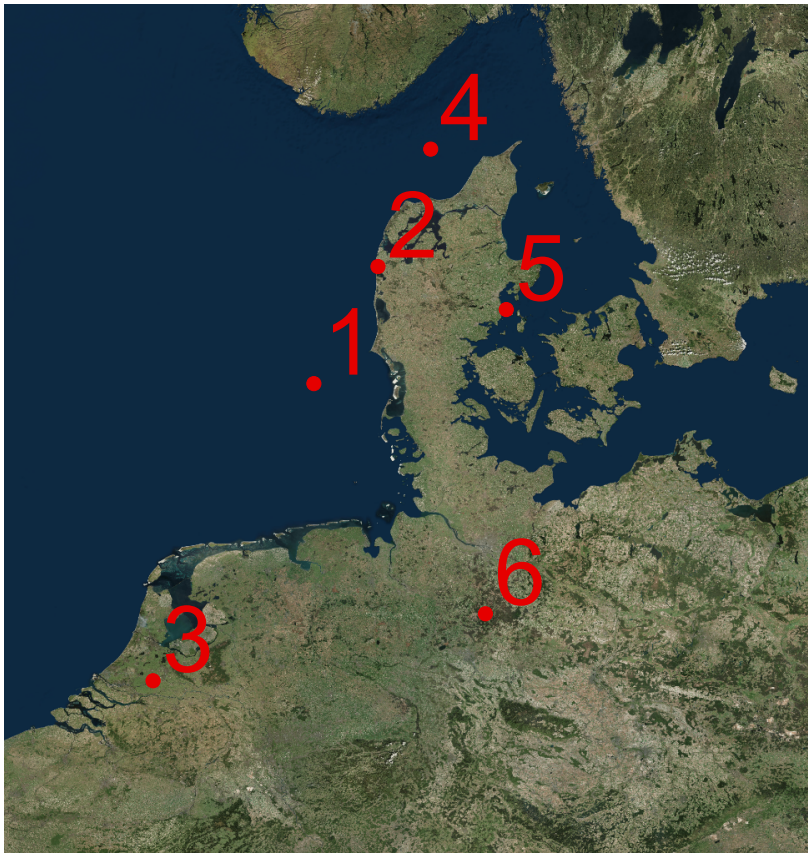

Figure 1. The six site locations: (1) FINO3, the North Sea. (2) Høvsøre, Denmark. (3) Cabauw, The Netherlands. (4) Dataless1, Skagerrak Sea. (5) Dataless2, Bay of Aarhus. (6) Dataless3, Germany.

The FINO3 site (Fabre et al., 2014) is a platform 80 kilometers off the coast of Denmark with a meteorological mast, reaching an elevation of 120 meters. Høvsøre (Peña et al., 2014) is a mast located approximately 2 kilometers from the coastline in western Jutland, Denmark. Apart from the sharp roughness-change represented by the coastline and the presence of a small enscarpment, the terrain can be characterized as homogeneous and flat. The Cabauw mast (Ulden and Wieringa, 1996) is located inland (40 kilometers to the coast) near the small towns of Cabauw and Lopik in the Netherlands. The surroundings are flat and fairly homogeneous agricultural fields, although some patches of forest and buildings are located in the surroundings. The Dataless1 site is located in the Skagerrak Sea approximately 50 kilometers off the northern coast of Denmark. Dataless2 is a site 5 kilometers offshore the east coast of Denmark, near the town of Aarhus. Besides the town and a small enscarpment the landscape is relatively flat and homogenous. Dataless3 is site north-east of the city of Bergen in northern Germany. The surrounding area is relatively flat and homogenous, however some small patches of forest are located nearby.

Wind Energ. Sci. Discuss., doi:10.5194/wes-2016-43, 2016
Manuscript under review for journal Wind Energ. Sci.
Published: 1 December 2016

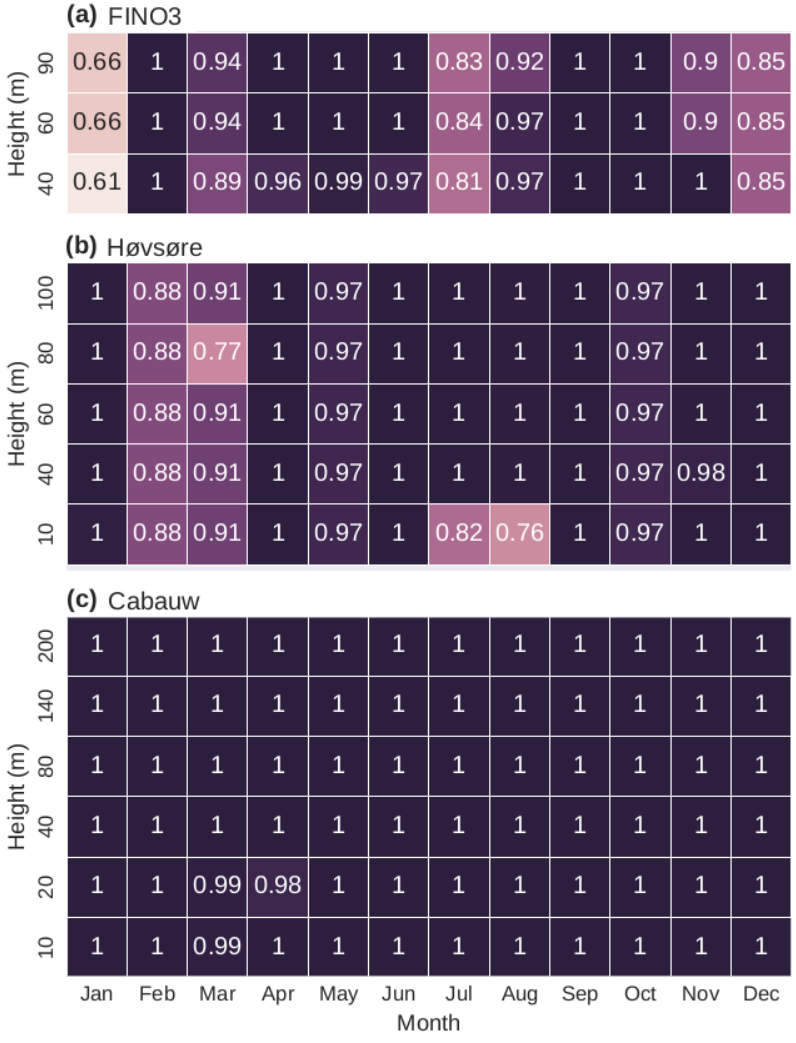

Figure 2. Availability of wind speed and direction data for FINO3, Høvsøre, and Cabauw given as a fraction of completeness for each month of the year 2011 for each comparison height.

The wind speed data availability for 2011 at the three meteorological masts is shown in Fig. 2. At Cabuaw the gaps were filled via interpolation due to the low abundance and magnitude of gaps (less than 2% missing data for any given month). This means that the gap-filled availability was 100%. The observations from the two other sites were not gap-filled. The intercomparison heights chosen for each site are shown for each site in Table A2, largely chosen because of the placements of instruments on the masts.

At FINO3 the wind speed measurements at three of the measurement heights: 50, 70, and 90 meters, comes from three separate booms with cup anemometers separated by a 120° angle. This is done to reduce effects of flow distortion from the

Wind Energ. Sci. Discuss., doi:10.5194/wes-2016-43, 2016
Manuscript under review for journal Wind Energ. Sci.
Published: 1 December 2016

tower on the wind speed measurements, by combining data from the three anemometors. However, two of the heights used in the intercomparison in this study, 40 and 60 meters, had only one cup anemometor available, so instead of using the single-anemometor data from 40 and 60 meters, the 50 and 70 meter data was vertically extrapolated down to 40 and 60 meters respectively, using log-law extrapolation in height. This was done under the assumption that the errors due to extrapolation are much smaller than those caused by flow distortion.

2.2 Submission procedure

The modelled time-series evaluated in this study were submitted by the participants to the open call for data issued by the European Wind Energy Association (EWEA). The submission procedure consisted of a template spreadsheet downloadable from the EWEA webpage, which included a questionnaire. The spreadsheet was filled with time-series of the required variables at each location and height. The questionnaire contained queries about the setup of the modeling system used. The participants then returned the spreadsheet to EWEA, whom passed it on to the authors in an anonymized version.

Table A3 shows the requested model variables. The questionnaire contained questions detailing the modeling setup, including information about the following: the model code and version, Surface Layer (SL) scheme, Planetary Boundary Layer (PBL) scheme, Land Surface Model (LSM), grid nests size(s) and spacing(s), vertical levels, landuse data, simulation and spin-up time, as well as initial and boundary conditions. Furthermore the participants were asked to comment on any additional modifications made to the model, as well as details on what assimilation, nudging, and ensemble methods used.

2.3 Models

The modeling groups participating with model data are listed in Table A4. There are representatives from companies, universities, research centres, and meteorological institutes. The represented models, including the different model setup options used, are shown in Table A5.

It is clear from Table A5 that the WRF model is the most used in this study, with 18 out of 25 groups using it. It is also clear that the Noah was the most popular LSM, and the Era-Interim Reanalysis the most popular source of boundary and initial conditions. The choice of PBL scheme and source of landcover data varied amongst the participants. The simulation length, including spinup time, of individual sub-simulation for most of the setups used was less than 100 hours, typically 12 hours of spin-up and 36 hours of total simulation. However, it did vary from 1 hour spin-up and 7 simulation up to continuously running for the full year.

As a source of reference, time series from the ERA-Interim reanalysis (Dee et al., 2011) was included in the comparisons whenever possible. The ERA-Interim reanalysis dataset is a global dataset based on extensive assimilation of surface and upper-air observations to the IFS global model using 4D-Var (Courtier et al., 1994). The spatial resolution of the dataset is approximately 80 km in the horizontal with 60 vertical levels, so bilinear interpolation was used for interpolation to the site locations. To get data on appropriate height levels linear interpolation in height was used. The dataset comes in 6 hour intervals at 0, 6, 12, and 18 Coordinated Universal Time (UTC), so linear interpolation in time was used to fill the sampling gaps.

Wind Energ. Sci. Discuss., doi:10.5194/wes-2016-43, 2016
Manuscript under review for journal Wind Energ. Sci.
Published: 1 December 2016

eawe european academy of wind energy
Open Access WIND ENERGY SCIENCE DISCUSSIONS

2.4 Statistical methods

This study was based on direct comparison between the observations and model output at collocated positions, as well as intercomparison between the output from the models. The sampling frequency for the study was chosen to be one hour. For the observation data this means hour mean values, while for the mesoscale models instantaneous values are used. This was done based on the assumption that the intra-hourly variance is low for the models, such that instantaneous values are very similar to the hourly means. To ensure temporal collocation, missing observations were used as a mask for the modeled output. Furthermore, to get vertically consistent profiles, only observations where all heights for a particular mast had available data were used. The model outputs submitted by the participants were assumed to be quality checked by the submitter, but it was also checked by the authors for obvious nonphysical or inconsistent behavior, and removed in that case.

From the variables presented in Table A3, the wind speed u and wind direction are the most important ones for wind energy applications and was emphasized the most. In the following, a subscript m will signify the temporal mean of that variable, i.e. u_m is the temporal mean wind speed. This is not to be confused with the mean value of the models, which we denote with a tilde, i.e. the model mean of temporal means is denoted $\tilde{u}_m$, and calculated as:

$$\tilde{u}_m = \frac{1}{N}\sum_{i}^{N} u_{m,i} \tag{1}$$

Here the index i is a reference to a specific model submission, and N is the number of models. Likewise it is useful to define the variation:

$$\tilde{\sigma}_{u_m} = \sqrt{\frac{1}{N}\sum_{i}^{N}\left(u_{m,i} - \tilde{u}_m\right)^2} \tag{2}$$

Here σ is the standard deviation, in this case of the intermodel variation between the temporal model means. Since $\tilde{u}_m$ and σ_{u_m} are sensitive to outliers, so the procedure applied in this study was:

1. Calculate $\tilde{u}_m$ and $\tilde{\sigma}_{u_m}$
2. Remove models where $|u_{m,i} - \tilde{u}_m|$ is greater than $3.5\tilde{\sigma}_{u_m}$
3. Recalculate $\tilde{u_m}$ and $\tilde{\sigma}_{u_m}$ with the new subset of models

This was done in an effort to reduce the sensitivity to the outliers. The value of 3.5 standard deviations was chosen somewhat arbitrarily to ensure that only somewhat 'extreme' outliers is removed. Only submission with data available at all heights was included in the calculation of the inter model mean and variation. This was done to get vertically consistent values.

2.4.1 Coefficient of variation

At the six sites used in this study the variation of wind speed σ_u scales with the mean wind speed u_m, so to allow for intercomparison of wind speed variation intensity across vertical levels the coefficient of variation $C_{v,u}$ was used. It is defined

Wind Energ. Sci. Discuss., doi:10.5194/wes-2016-43, 2016
Manuscript under review for journal Wind Energ. Sci.
Published: 1 December 2016

eawe european academy of wind energy
Open Access WIND ENERGY SCIENCE DISCUSSIONS

as the variation over the mean σ_u/u_m, and is a unit-less measure of the relative variation at the sampling time scale. At timescales of seconds it is known as turbulent intensity, but in this case, with a sampling frequency of one hour, it represents the intensity of variations of synoptic- and mesoscale weather phenomena.

2.4.2 Wind speed shear exponent

The shear exponent (α) given by eq. (3) provides a measure of the relative change of wind speed with height between to levels z_1 and z_2.

$$\alpha = \frac{\ln\left(\frac{u_1}{u_2}\right)}{\ln\left(\frac{z_1}{z_2}\right)} \tag{3}$$

In the surface layer α is strongly influenced by the surface roughness and the atmospheric stability. It is important that the mesoscale models capture the distributions of α well, because it is an indirect measure of how well the mesoscale models capture the local effects of roughness and stability.

2.5 Wind energy application

To investigate the errors and spread of the models for simple applied wind energy applications, the models output were used for a wind resource assesment exercise.

A typical approach to resource assessment in the wind energy sector is to run a mesoscale model in the area of interest for a number of years, followed by a downscaling process where the wind climate statistics obtained from the mesoscale model is used as input for a microscale model (Badger et al., 2014; Hahmann et al., 2015). In simple terrain the microscale model usually consists of a simple flow model, similar to the Wind Applications and Analysis Program (WAsP). WAsP uses a linearised flow model based on the principles of Jackson and Hunt (1975), and consists of an upscaling procedure where local effects from variations in orography, surface roughness, and objects, are removed from the wind climate statistics. This is referred to as 'generalisation' of the wind climate, and the generalized statistics are representative for a larger surrounding area than the site specific wind climate. The size of the area that it represents depends on the complexity of that area. The generalised wind climate can then be downscaled to a specific site of interest by 'reversing' the generalization process, i.e. putting back in the site specific effects of orography, surface roughness, and objects.

Given a downscaled wind climate and a turbine-specific power curve, the expected power output can then be calculated. Since the participants in this intercomparison did not submit their model-specific orography and roughness maps, it is not possible to go through the generalization procedure, and downscaling process at the inland sites. However, for the offshore site FINO3 there are no effects of orography, and if differences in surface roughness is assumed to negligible between the models, then the downscaling process can be applied without the generalization. This was done for the FINO3 site at 90 meters, assuming a single Vestas V80 turbine(s) at the site, and then repeated for the wind farm of Horns Rev, which is a 80 turbine large wind farm located near FINO3. This was done using the simple wake parameterization in the WAsP model to study how wake effects can alter the results.

Wind Energ. Sci. Discuss., doi:10.5194/wes-2016-43, 2016
Manuscript under review for journal Wind Energ. Sci.
Published: 1 December 2016

eawe european academy of wind energy
Open Access WIND ENERGY SCIENCE DISCUSSIONS

3 Results

3.1 Mean quantatives

3.1.1 Mast sites

From the vertical profiles of mean wind speed (u_m), presented in Fig. 3, it is clear that at the offshore site FINO3 most mesoscale models (MM) underpredict u_m at the three heights. However, the bias is less than $0.27\,\mathrm{m/s}$ on average, corresponding to about 2.8%, which is a small number, especially compared to the ERA-Interim data, which shows a larger negative bias than all of the mesoscale models. The intermodel variance $\tilde{\sigma}_{u_m}$ at FINO3 is $2.7 - 3.1\%$, decreasing with height, which is the lowest combined inter-model variance of any of the six sites.

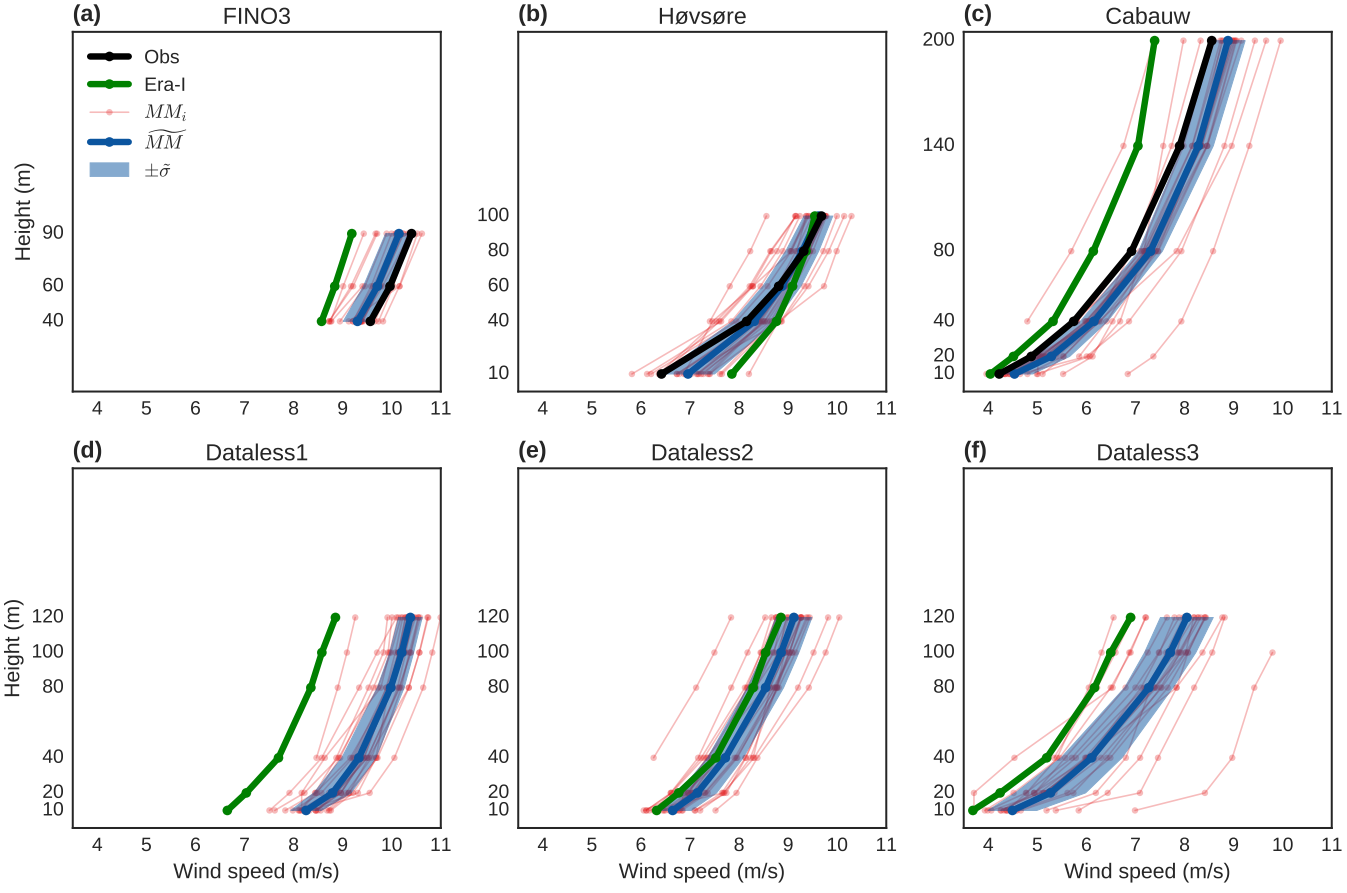

Figure 3. Vertical profiles of mean wind speed (u_m), for all of 2011, at the six sites, for: the observations (black), the ERA-Interim dataset (green), the Mesoscale Models MM_i (red), and the mesocale models mean and intermodel variance $\widetilde{MM} \pm \tilde{\sigma}$ (blue).

Wind Energ. Sci. Discuss., doi:10.5194/wes-2016-43, 2016
Manuscript under review for journal Wind Energ. Sci.
Published: 1 December 2016

eawe european academy of wind energy
Open Access WIND ENERGY SCIENCE DISCUSSIONS

At Høvsøre the mesoscale models and ERA-Interim generally have small wind speed biasses above 10 meters, showing a bias of the mesoscale model mean $\tilde{u}_m$ that is smaller than $\pm 0.16\,\mathrm{m/s}$ ($< \pm 1.9\%$), and a intermodel variance is $3.0 - 5.2\%$, decreasing with height, which is low compared to the other sites. At 10 meters the mesoscale models generally overpredict the mean wind speed and the model mean wind speed $\tilde{u}_m$ has a positive bias of $0.54\,\mathrm{m/s}$ ($\sim 8.41\%$). ERA-Interim also overpredicts the mean wind speed at 10 meters, with an even larger bias than $\tilde{u}_m$, and the largest intermodel variance is also observed there (7.8%).

At Cabauw most of the mesoscale models overpredict u_m. Only one of the mesoscale and the reanalysis datasets, shows a significant underprediction, and in the case of the reanalysis this underestimation increases with height. The overprediction by the rest of the mesoscale models varies in magnitude, but the average of the models, excluding the outliers, are in the range $4 - 9\%$ for the different heights, with the largest relative errors near the surface. The inter model variance ($\tilde{\sigma}_{u_m}$) at Cabauw vary between $3.3 - 8.1\%$ at the different heights, and is highest at the lowest levels.

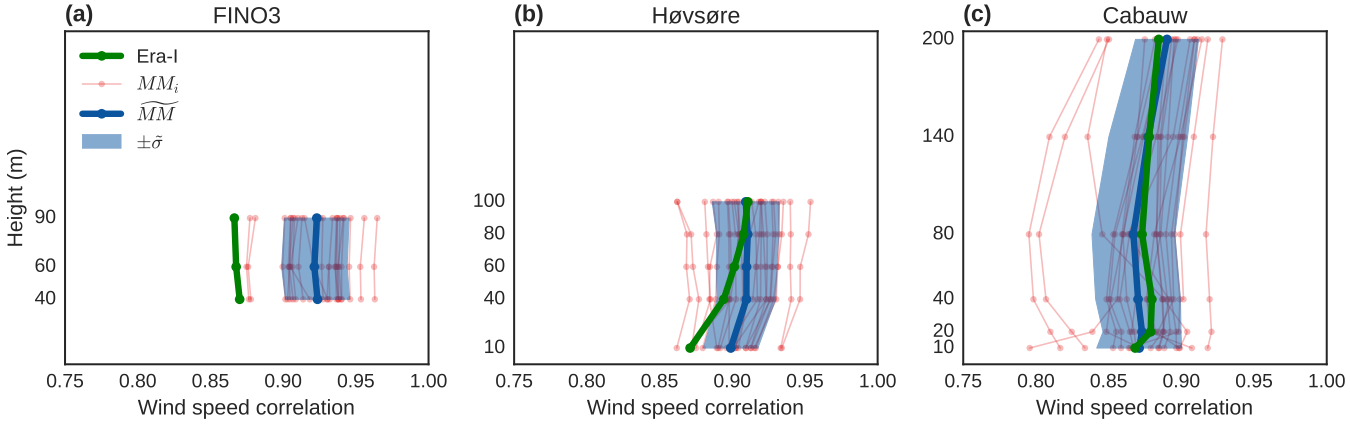

Figure 4. Vertical profiles of correlation coefficient between model and observation for wind speed for all of 2011 at the three mast sites, for: ERA-Interim (green), the mesoscale models MM_i (red), and the mesoscale models mean and intermodel variance $\widetilde{MM} \pm \tilde{\sigma}$ (blue).

Wind speed correlation coefficients between the models and the observations are shown in Fig. 4. The figure reveals that the correlation between the mesoscale models and the observations, on an hourly time scale is > 0.8. It is also clear that correlation is generally higher at FINO3, and slightly lower at Høvsøre and Cabauw. At Høvsøre and Cabauw the correlation decrease with height. The correlation of the reanalysis data is similar to the mesoscale models at Cabauw and aloft at Høvsøre, but slightly lower at FINO3 and at the lowest levels at Høvsøre. The intermodel variance is $\approx 2.5\%$ everywhere, by at Cabauw, especially at the lowest levels, it is slightly higher ($\approx 3.4\%$).

The mean coefficient of variation ($C_{v,u}$) for wind speed is shown in Fig. 5 for all six sites. It shows that at FINO3 the average of the mesoscale models $\tilde{C}_{v,u}$ is similar to the the observations, the difference is less than 1% at all three heights. Ignoring one outlier, the intermodel variance range between $3.0 - 3.5\%$ at the three heights. The outlier with much lower values is due to lower variance for that particular model not due to any significant difference in the mean wind speed compared to the

Wind Energ. Sci. Discuss., doi:10.5194/wes-2016-43, 2016
Manuscript under review for journal Wind Energ. Sci.
Published: 1 December 2016

other models. It was removed by the filtering method described in sect. 2.4 in the calculation of the models mean ($\tilde{C}_{v,u}$) and inter-model variance ($\tilde{\sigma}_{C_{v,u}}$). The ERA-Interim dataset also captured the magnitude of $C_{v,u}$ well at FINO3, showing values similar to the observations and the mesoscale models.

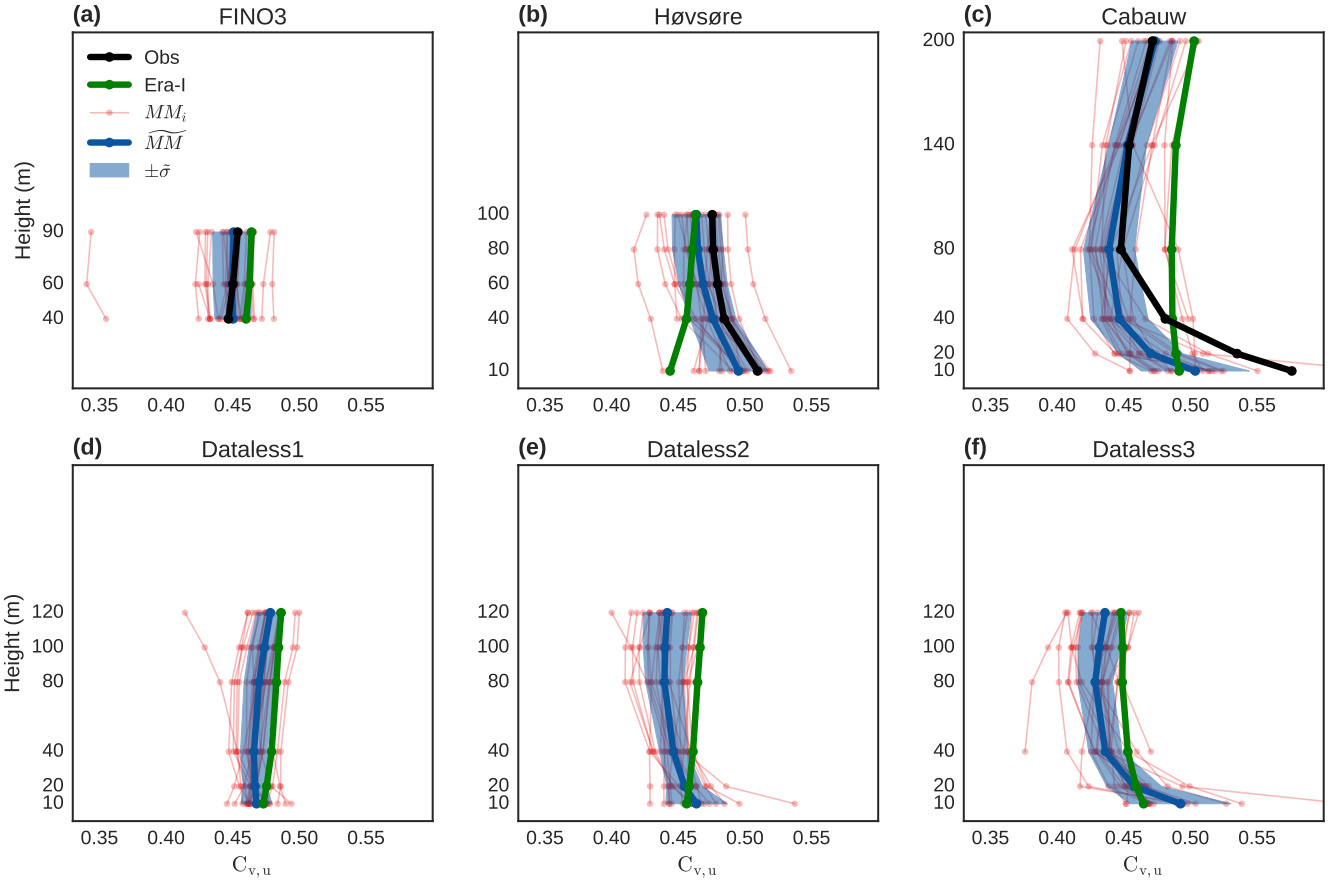

Figure 5. Vertical profiles of coefficient of variation for wind speed $C_{v,u}$ for all of 2011 at the six sites, for: observations (black), ERA-Interim (green), the mesoscale models MM_i (red), and the mesoscale models mean and intermodel variance $\widetilde{MM} \pm \tilde{\sigma}$ (blue).

At Høvsøre $C_{v,u}$ decreases with height for both the observations, and most of the mesoscale models. The model average ($\tilde{C}_{v,u}$) agrees well with the observations, but underestimates it by about 2%. The ERA-Interim dataset does not capture the behavior, and instead show an increase with height, but at the highest levels it does agree quite well with the model average and observation values. The spread of the mesoscale models ($\sigma_{C_{v,u}}$) is slightly higher than at FINO3 ($3.6 - 4.4\%$), highest at the surface.

The magnitude of $C_{v,u}$ is largest across all sites at 10 meters at Cabauw. Above 10 meters a sharp drop-off with height up to 80 meters is observed, followed by a small increase up to 200 meters. Most of the mesoscale models are able to capture this behavior, which is reflected in the mean of the models ($\tilde{C}_{v,u}$). However, the models underestimate the magnitude and the

Wind Energ. Sci. Discuss., doi:10.5194/wes-2016-43, 2016
Manuscript under review for journal Wind Energ. Sci.
Published: 1 December 2016

drop-off of $C_{v,u}$ at the lowest levels, at 10 and 20 meters the bias of the average of the mesoscale models is $\approx 12\%$. Above 80 meters the mean of the models and observations agree quite well. The ERA-Interim dataset do not show much change with height, and tend to overestimate $C_{v,u}$ above 40 meters, and underestimate it below. The inter-model variance ($\tilde{\sigma}_{C_{v,u}}$) of the mesoscale models is largest at the lowest levels, 8.0% at 10 meters, and gradually decreases to less than 4% at 200 meters.

3.1.2 Dataless sites

The mesoscale models mean wind speed (u_m) at the three Dataless sites (Fig. 3 d, e, and f) reveals that at the offshore site Dataless1 the mesoscale models have a larger mean wind speed than the reanalysis, similarly to the FINO3 offshore site. The intermodel variance $\tilde{\sigma}_{u_m}$ is $2.3 - 4.3\%$ with the largest variance found at the lowest levels.

At the Dataless2 site, offshore the coast in Denmark, the mesoscale models and the reanalysis data agree quite well, but the mean wind speed of the reanalysis data are slightly lower than the average of the mesoscale models. The inter model variance ($\tilde{\sigma}_{u_m}$) at the site is 5.7% at 10 meters, and gradually decrease to 4.0% at 120 meters.

At the Dataless3 site the mean wind speed of the reanalysis data is generally lower than the mean wind speed from the mesoscale models. The magnitude of this difference is larger aloft. The site also shows the largest inter-model variance of any of the six sites: $10.1 - 13.6\%$ at 10 - 40 meters, and $6.7 - 6.8\%$ at 80 - 120 meters. One mesoscale model show considerably larger mean wind speed than the rest, but was not included in the calculation of the model mean and variance.

The coefficient of variation at the three Dataless sites is presented in Fig. 5 (d), (e), and (f). It shows that relative variations are larger at Dataless1 than at FINO3, but there is a good agreement between the mesoscale models ($\tilde{\sigma}_{C_{v,u}}$ is $< 2.5\%$). The ERA-Interim dataset show a large coefficient of variation compared to most mesoscale models, but not significantly.

The coefficient of variation at Dataless2 is slightly lower than for Dataless1 and decrease with height for most mesoscale models, but not for the ERA-Interim dataset. The inter-model variance is comparable to that at Høvsøre ($2.3 - 5.0\%$) and is also slightly higher at the lowest levels.

At Dataless3 large values of coefficient of variation for wind speed is observed at the lowest levels, similar to Cabauw, and a sharp drop-off with height up to 40 meters is also seen. Just like at Cabauw, ERA-Interim do not show the drop-off with height. The mesoscale models have a stronger agreement at Dataless3 than at Cabauw ($2.9 - 4.8\%$), but show the largest srpead at 10 meters, exactly like for Cabauw.

In general the observed behavior at the Dataless sites for both mean wind speed and coefficient of variation for wind speed is very similar to the behavior observed at each of counterpart-sites with observations, apart from a slightly better agreement between the mesoscale models at low levels at the Dataless2 than at Høvsøre, and less agreement amongst the models at the Dataless3 site compared to Cabauw, but it is probably a reflection of differences in terrain-complexity of the sites.

3.2 Distributions

Figure 3 shows that the mesoscale models generally capture the mean wind speed well. In the following the ability of the models to reproduce distributions of wind direction (Fig. 6), wind speed (Fig. 7), and shear exponent (Fig. 8) is demonstrated. The distributions are presented at heights relevant to wind energy applications, between 80 and 90 meters, and in the case

Wind Energ. Sci. Discuss., doi:10.5194/wes-2016-43, 2016
Manuscript under review for journal Wind Energ. Sci.
Published: 1 December 2016

eawe european academy of wind energy
Open Access WIND ENERGY SCIENCE DISCUSSIONS

of wind shear exponent, between 40 meters and 80-90 meters. In the following only the sites with observations have been included, because the results at each of the three data-less sites are similar to the results from the corresponding site with observations (offshore, coastal, inland).

The wind roses (distribution of the wind direction), shown in Fig. 6 in 15° sectors at heights of either 80 or 90 meters, reveal that the models capture the observed distributions well, and the intermodel variance is low. In all three cases the mesoscale models have captured the distribution better than the reanalysis data does.

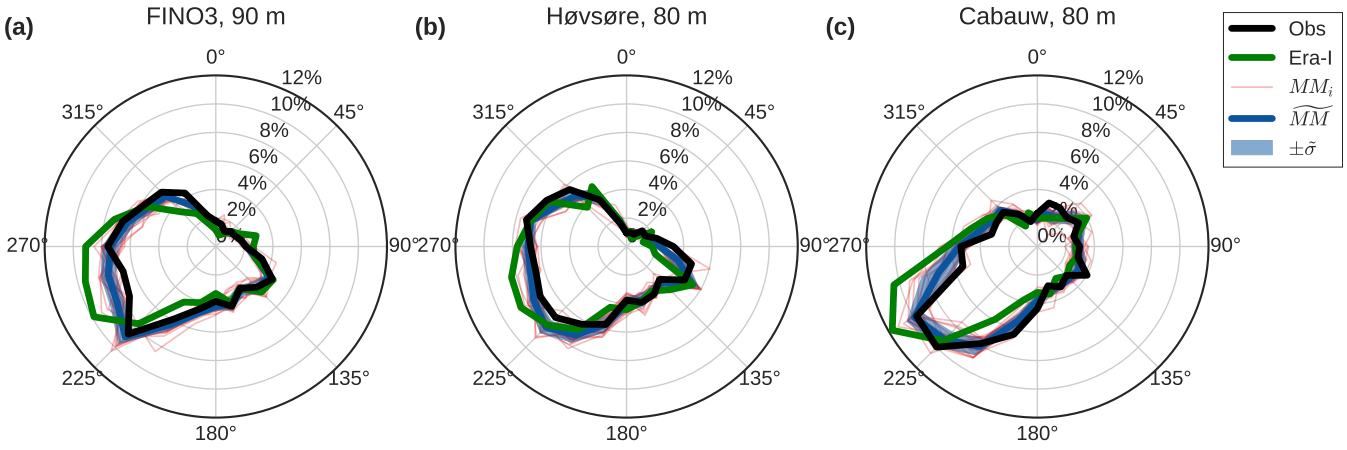

Figure 6. Distributions of wind direction at the six sites based on 24 directions, each representing 15°, for: the observations (black), the ERA-Interim dataset (green), the Mesoscale Models MM_i (red), and the mesocale models mean and intermodel variance $\widetilde{MM} \pm \tilde{\sigma}$ (blue).

Wind speed distributions (Fig. 7) show that on average the mesoscale models capture the distributions well, apart from a slight shift towards the higher wind speeds at Cabauw, resulting in the positive bias in mean wind speed observed in Fig. 3. The ERA-Interim dataset capture the distribution well at Høvsøre, but show a distribution shifted towards lower windspeeds at FINO3 and Cabauw.

The distributions of the shear exponent (α) for the three mast sites are presented in Fig. 8. Under neutral conditions and a uniform surface roughness (for all wind directions) a sharp distribution centered around a single α value should be observed, so for offshore sites like FINO3 the spread in shear exponent comes from variations in the atmospheric stability, the Fig. reveals that in that particular case the models capture stability well on average at the site. The ERA-Interim dataset however, do not seem to capture the strongest shear situations.

At Høvsøre and Cabauw the distribution of α is a combined effect of both the upstream surface roughness, which cannot be expected to be uniform (it varies with direction), and the varying atmospheric stability. For example, one would expect that at the coastal site Høvsøre the upstream roughness vary a lot depending on whether the wind is coming from land or sea, something that was also observed by Hahmann et al. (2014b). The figure shows that while the distributions are generally well captured, a slight shift towards lower shear is observed at both sites. The ERA-Interim dataset does not capture the strong shear cases at Høvsøre, and at Cabauw neither the weak or strong shear cases are sufficiently represented. Part of the reason for the

Wind Energ. Sci. Discuss., doi:10.5194/wes-2016-43, 2016
Manuscript under review for journal Wind Energ. Sci.
Published: 1 December 2016

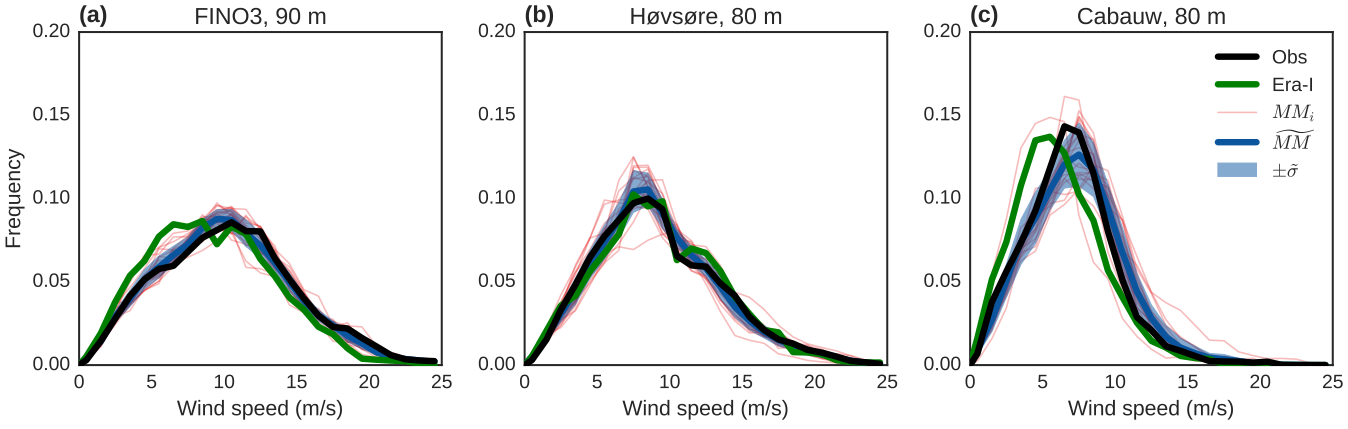

Figure 7. Distributions of wind speed at three mast sites, for: the observations (black), the ERA-Interim dataset (green), the Mesoscale Models MM_i (red), and the mesocale models mean and intermodel variance $\widetilde{MM} \pm \tilde{\sigma}$ (blue).

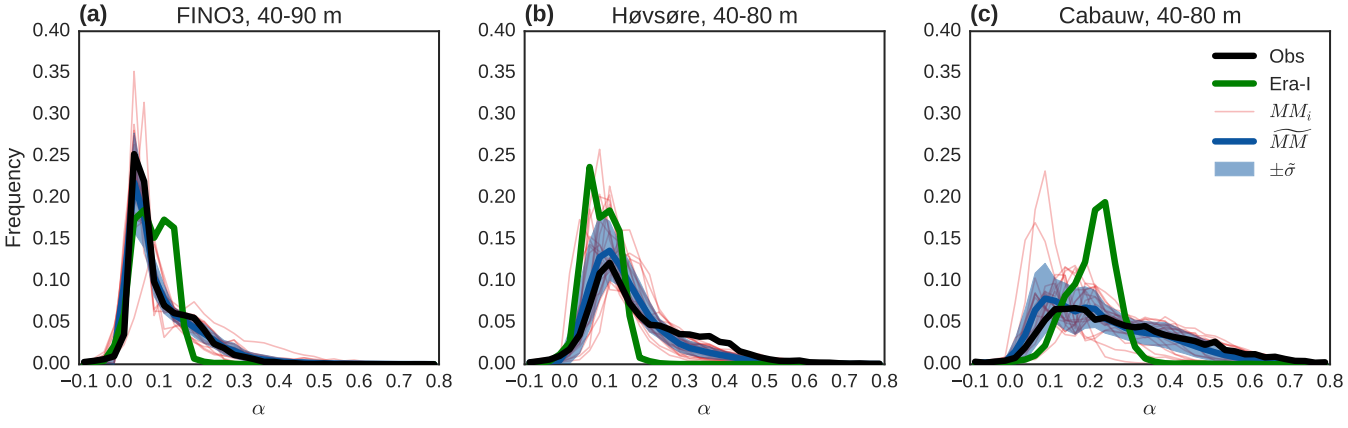

Figure 8. Frequency of occurance of the shear exponent (α) at the three mast sites, for: the observations (black), the ERA-Interim dataset (green), the Mesoscale Models MM_i (red), and the mesocale models mean and intermodel variance $\widetilde{MM} \pm \tilde{\sigma}$ (blue).

Wind Energ. Sci. Discuss., doi:10.5194/wes-2016-43, 2016
Manuscript under review for journal Wind Energ. Sci.
Published: 1 December 2016

eawe european academy of wind energy
Open Access WIND ENERGY SCIENCE DISCUSSIONS

poor results for ERA-Interim is the linear interpolation from model levels to fixed height levels used in the data extraction. However, at least three model levels were used in the interpolation to the two height levels (40 and 80 meters), so even though some dampening of the shear coefficient is expected from the interpolation method, it does not fully explain the poor results.

3.3 Effect of upstream conditions on variation of wind speed

In order to investigate whether a dependency on upstream conditions exists for the coefficient of variation for wind speed (shown in Fig. 5) exists, two of the sites were studied. One offshore (FINO3), representing the isotropic upstream surface roughness case, and one with a nearby coastline going from south to north (Høvsøre), represeting the case with a strong surface roughness dependence on direction. The coefficients of variation was binned according to four wind directions representing 90 degree sectors: north, east, south, and west. The values for the east and west sectors at the two sites was then extracted and analyzed.

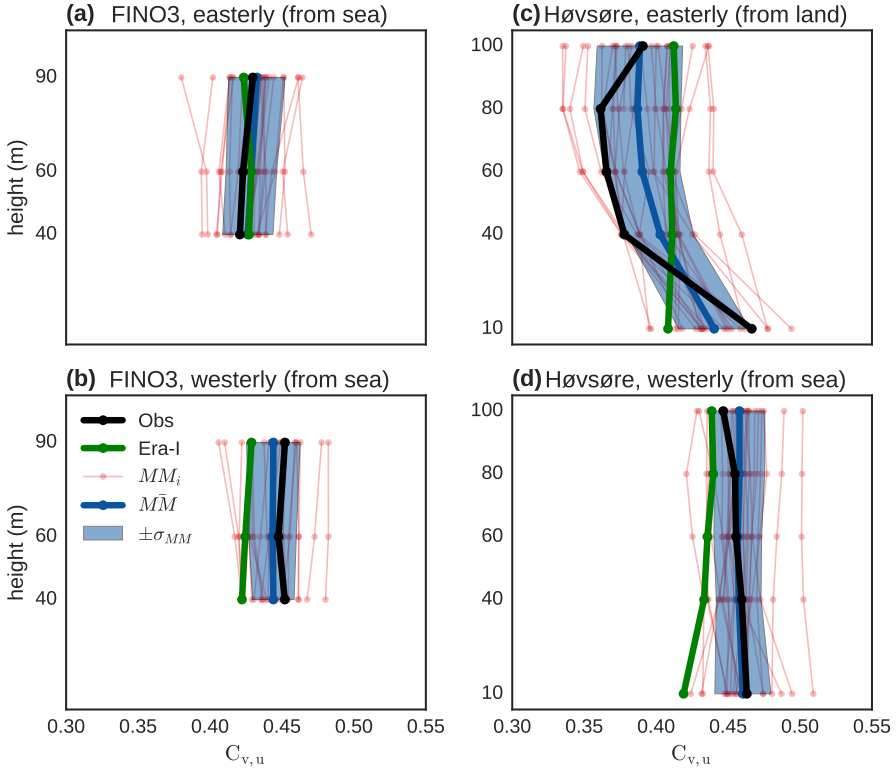

Figure 9. Coefficient of variation for wind speed $C_{v,u}$ for split into westerly and easterly flow at FINO3 (a,b) and Høvsøre (c,d), for: the observations (black), the ERA-Interim dataset (green), the Mesoscale Models MM_i (red), and the mesocale models mean and intermodel variance $\widetilde{MM} \pm \tilde{\sigma}$ (blue).

Wind Energ. Sci. Discuss., doi:10.5194/wes-2016-43, 2016
Manuscript under review for journal Wind Energ. Sci.
Published: 1 December 2016

eawe european academy of wind energy
Open Access WIND ENERGY SCIENCE DISCUSSIONS

Figure 9 shows the two cases for FINO3 and Høvsøre. At FINO3 the coefficient is slightly lower for easterly flow for both the models and observations, and no dependence on height is observed. The sample size is smaller for easterly directions, about half that of westerly directions, but both sample size are large (N > 1000) so the difference in $C_{v,u}$ due to differences in sample sizes is expected to be small. For both wind directions the average of the mesoscale models, and ERA-Interim, captures the observed behavior well, and the inter-model variance for the mesoscale models is similar for both directions. At Høvsøre westerly flow comes from the sea, and easterly from land. The figure shows that wind sectors coming from sea at Høvsøre have a higher coefficient of variation compared to the land sector. Easterly winds (coming from land) show larger coefficients of variation at the lowest levels, which decreases with height. This reduction with height is underestimated by most of the mesoscale models, and completely missed by the ERA-Interim dataset. For westerly winds (coming from the sea) at Høvsøre the models and observations agree almost exactly.

The westerly wind sector at Høvsøre, where the wind comes from the sea, show a very similar pattern to the two sectors at FINO, that is: no change with height. This points to the fact that the pattern observed for the easterly wind directions at Høvsøre, where a clear dependence on height is observed, is due to influence from the upstream surface conditions. These influences do not appear to be well captured by the ERA-Interim dataset, but the mesocale models are, to some degree, able to capture them.

3.4 Individual model performance

The previous sections have been focused on distributions, mean quantities, and the variance of the mesoscale models. In this subsection the attention is on identifying the things that set the models apart, be it due to the chosen parametrization, the dataset used for initial and boundary conditions, the setup of the grid, the time integration choice, or otherwise.

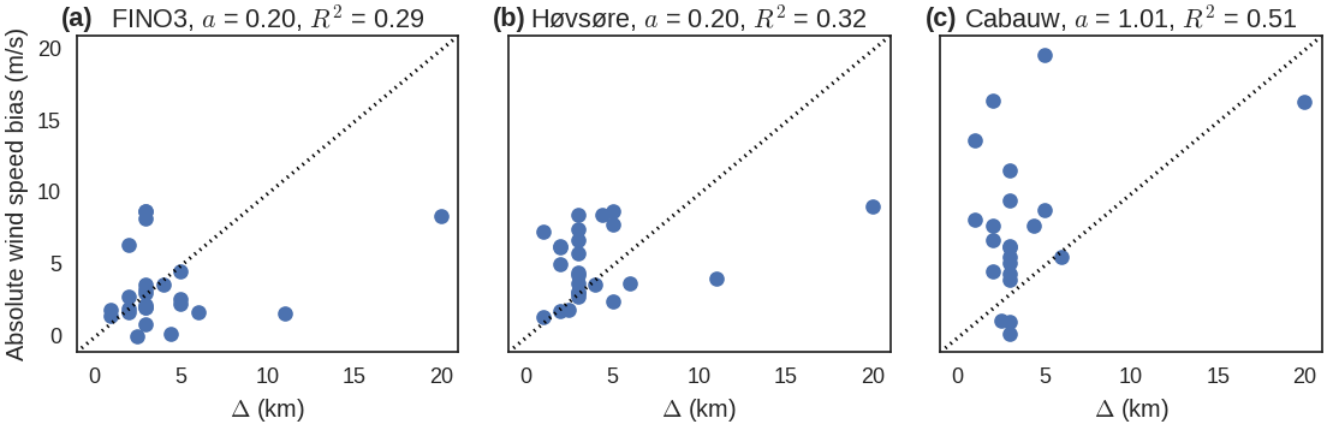

Figure 10. Absolute mean wind speed bias at 40 meters vs. model resolution for three sites with a mast. R^2 is the correlation coefficient, and a is the slope of a least-squares fit to the data points.

Wind Energ. Sci. Discuss., doi:10.5194/wes-2016-43, 2016
Manuscript under review for journal Wind Energ. Sci.
Published: 1 December 2016

eawe european academy of wind energy
Open Access WIND ENERGY SCIENCE DISCUSSIONS

The hypothesis of this study was that, given enough samples (models) in the study, it would be possible to identify the statistical effects of choosing a particular model setup, compared to another.

The following factors were hypothesised to influence the surface layer winds:

- The model grid spacing and source of orography and land use data, due to the importance of accurately representing the orography and the upstream surface roughness.
- The choice of SL and PBL scheme.
- To a lesser degree: the model, the boundary and initial conditions, the spin-up and simulation time, and the domain placement.

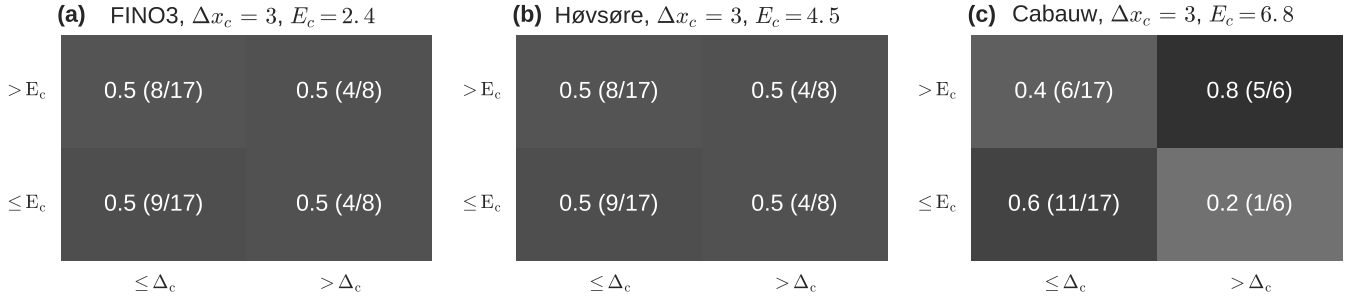

Figure 11. Chance of mesoscale models to have a mean wind speed error (E_c) larger or smaller than the median error if they have smaller or larger grid spacing than the median (Δ_c) for the three mast sites at 40 meters.

The hypothesized correlations were investigated using a number of approaches, and although some weak indications of correlation between the model grid spacing and the absolute wind speed bias (Fig. 10), no significant correlation were found between the different performance metrics tested for the surface layer winds and the factors listed above.

Figure 11 shows the chance, for a random model, of having a mean wind speed error (E_c) that is larger or smaller than the median error, depending on whether the model grid spacing is larger or smaller than the median model grid spacing (Δ_c), for the three mast sites at 40 meters. At FINO3 and Høvsøre the chance of a lower than median error is the same, whether the model grid spacing is larger or smaller than the median spacing. At Cabauw a higher chance of a smaller mean wind speed error is observed for smaller grid spacing, and a higher chance for larger errors is seen for larger grid spacing.

3.4.1 Performance consistency across sites

To investigate whether the models that perform well at one site also perform well at the other sites, the mean wind speed error, as well as the wind speed correlation with observations, was compared for site-wise pairs, see Fig. 12. The figure reveals that for wind speed correlation (Fig. 12 b) a clear connection is seen between the correlation at one site and the correlation at another, for all site pairs, resulting in a coefficient of determination R^2 of 0.57 or above for the three site-pairs. For mean

Wind Energ. Sci. Discuss., doi:10.5194/wes-2016-43, 2016
Manuscript under review for journal Wind Energ. Sci.
Published: 1 December 2016

eawe european academy of wind energy
Open Access WIND ENERGY SCIENCE DISCUSSIONS

wind speed error (Fig. 12 a) the correlation between FINO3 and Høvsøre ($R^2 = 0.63$), and FINO3 and Cabauw ($R^2 = 0.65$) is quite high, while it is smaller for Høvsøre and Cabauw ($R^2 = 0.44$). Even though a correlation is observed between the performance at one site, and another, for these two metrics, two things should be kept in mind: 1) It is not always the same models that perform well for mean wind and for wind speed correlation 2) the temporal correlation between the sites is quite high, Mehrens et al. (2016) showed that for sites in the North Sea area the temporal correlation of 10 minute average wind speed measurements is $R^2 \approx 0.5$ at distances up to 500 km, which makes it difficult to quantify and separate the effects from the temporal correlation and from and the model skill. The sites are between 150 and 550 kilometers from each other, so some temporal correlation should be expected.

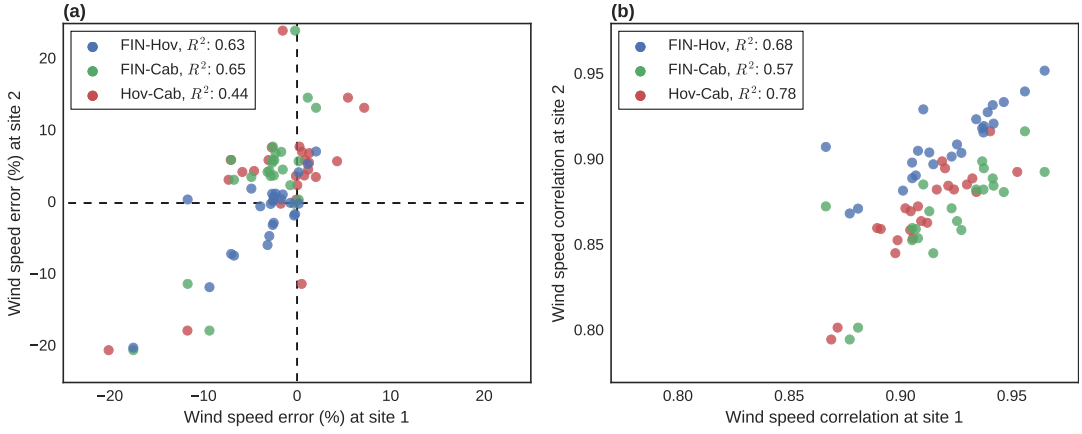

Figure 12. a) Errors of u_m at one site for the models plotted against the error of u_m at another site for the same model. b) Correlation of u at one site plotted against the correlation of u at another site. The coefficient of determination R^2 is shown for the different site-pairs in the legends. In both a) and b) the height is 80 meters for Høvsøre and Cabauw, and 90 meters for FINO3.

3.5 Wind energy application

The mesocale model timeseries was applied to a simple wind energy resource assessment application using the 90 meter data at the offshore site FINO3, as described in section 2.4. In figure 13 the error of the calculated mean wind speed u_m, mean power density P_m, mean power density with an assumed power curve $P_{m,pc}$, and the mean power density of 80 turbines in a wind farm including wake effects $P_{m,wf}$.

A majority of the models shown in Fig. 13 have less than $\pm 5\%$ error for mean wind speed. The errors are mostly due to an underestimation of the mean wind speed, and for some of them severely ($< 10\%$). For mean power density the spread of the models are, as expected, much larger due to the third power dependence on the wind speed. However, when the power density is calculated using a turbine power-curve, where the highest wind speeds (> 14 m/s) are less important for the power than it is for power density, the variance is comparable to the variance for mean wind speed. For the wind farm situation, where the power density is dependent on the wind direction distribution, and the losses due to wake effects, the variance is comparable in

Wind Energ. Sci. Discuss., doi:10.5194/wes-2016-43, 2016
Manuscript under review for journal Wind Energ. Sci.
Published: 1 December 2016

eawe european academy of wind energy
Open Access WIND ENERGY SCIENCE DISCUSSIONS

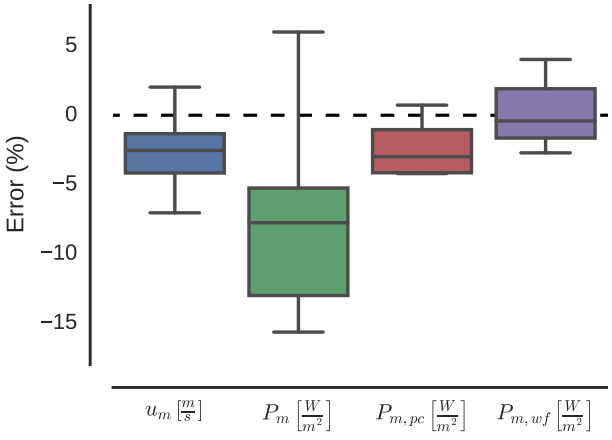

Figure 13. Distributions of errors from the models output at 90 meters at FINO3 for the following statistical quantaties: 1) the mean wind speed u_m (blue), 2) power density P_m (green), 3) power density with an implied power curve $P_{m,pc}$ (red), and 4) average power density of a wind farm including the same implied power curve as 3) and wake effects (purple). Outliers are not shown, but the most extreme ones go to -60% for P_m, -37% for $P_{m,wf}$, -35% for $P_{m,pc}$, and -25% for u_m.

size to that of mean wind speed and $P_{m,pc}$, and most models have errors smaller than $\pm 2\%$. The improvement seen for $P_{m,wf}$ is caused by a underestimation of the wake effects for most models, leading to a relative increase in mean power density, offsetting the underprediction from the modelled wind speed distribution.

4 Discussion

The increase of both model errors and inter-model variance, observed with decreasing height at the inland sites, indicates an influence of misrepresentation of surface characteristics, such as surface roughness and orography of the models, and it highlights the need for downscaling of the mesoscale results, to include high resolution information and microscale effects, especially if the models are used for siting and resource assessment.

While the current study offered great insight, especially into the inter-model variance of mesoscale models, several things could be improved in future studies, including: 1) The model representation of surface roughness for the nine grid cells closest to the site of interest, was submitted by less than half of the participants. In future studies having these details for all models may help detect misrepresentation of the surface characteristics. 2) A larger sample size would improve the robustness of the statistics, and allow for more grouping of the model output, which may allow for a formulation of best-practice principles for NWP modeling for wind energy. 3) This study showed that for offshore sites the model errors and inter-model variance is quite low, so future studies would probably benefit most from focusing on inland sites of low to moderate complexity where effects from the surface characterisation in the model can be studied in greater detail. 4) Future studies could also focus on specific cases, or phenomena, that is important for wind energy, for example Low Level Jets (LLJ). Several studies, e.g. Storm

Wind Energ. Sci. Discuss., doi:10.5194/wes-2016-43, 2016
Manuscript under review for journal Wind Energ. Sci.
Published: 1 December 2016

et al. (2009), have shown that the PBL schemes used used in most mesoscale models, including YSU, MYJ, and MYNN have difficulties in accurately capturing surface layer winds in stable conditions, including LLJ's. Capturing LLJ's can be of vital importance because they are associated with strong winds, strong shear, and high turbulence levels, which have the potential to either increase power output, or damage the turbine, depending on the strength and location of the jet.

5 Summary and conclusions

In this paper an intercomparison of results from 25 different NWP models has been presented for six locations characterized by simple terrain in Northern Europe. The models were compared with each other and, at three of the sites, with observations from nearby meteorological masts for the year 2011. The results, including model meta-data, was submitted by modeling groups from the wind energy sector, and the model setups represent the practice used within the industry today.

The study showed that on average the mean wind speed as estimated by the mesoscale models had low biases ($< 3\%$) at the offshore site FINO3 and above 10 meters at the coastal site of Høvsøre, meanwhile the largest biases ($7 - 9\%$) was observed at the lowest levels at Høvsøre (10 meters) and Cabauw (10 and 20 meters). A similar pattern existed for the model spread, which was greater at the lowest levels and smaller aloft, and largest at inland and coastal sites, and smaller offshore. The same pattern was also present for correlation between modeled and measured wind speed at the three mast sites: weaker correlation inland and closer to the surface.

The coefficient of variation (σ/u) was used assess how well the models are able to capture the relative wind speed variation. It revealed that the average of the models have biases of less than 3% at FINO3, Høvsøre, and above 40 meters at Cabuaw, but at 10-40 meters at Cabauw the biases was $7 - 13\%$ due to a large coefficient of wind speed variation at the lowest levels, that decrease with height, that is not well captured by the models.

The study also showed that for the distribution of wind direction (wind rose) only small deviations between the mesoscale models and the observations are seen. For wind speed, the models also represent the distributions accurately, apart from a slight shift towards the high wind speeds at Cabauw. For distributions of the shear exponent (α), which reflects the ability of the models to accurate estimate the combined effects of surface roughness and atmospheric stability, the models do well at FINO3, but seem unable to capture all cases of strong shear at Høvsøre and Cabauw.

A detailed study of FINO3 and Høvsøre showed that for wind directions coming from sea the coefficient of variation for wind speed is constant with height, and the models capture the magnitude and behavior well, while for wind directions coming from land at Høvsøre the coefficient is dependent on height. On land the observed coefficient of variation was generally lower, and the models were less accurate, compared to wind directions coming from sea.

Strong evidence was found, for some metrics (mean wind speed, correlation), that the model performance was consistent between site-pairs for the mast sites. However, since the mast sites are located within a distance where some spatial correlation is expected, the consistency cannot be exclusively contributed to the model skill.

A wind energy case study was made at FINO3, where the observations and the output from the models output was used to estimate the power output for one single turbine and for a whole wind farm that included wake effects. The study showed that

Wind Energ. Sci. Discuss., doi:10.5194/wes-2016-43, 2016
Manuscript under review for journal Wind Energ. Sci.
Published: 1 December 2016

while a large spread exists between the modeled power density, it is reduced when the power is calculated via a power-curve. It also showed the importance of accurately estimating the wind speed distribution, since the small deviation in the distributions changed the power distribution strongly.

While it was a key objective of this study to determine the model setup choices that have a large impact on the models ability to estimate the wind climate accurately in the lowest part of the PBL, only weak indications were found.

6 Data availability

The output data from the mesoscale models have been submitted submitted to the European Wind Energy Association (EAWE) for the mesoscale benchmarking study under an agreement that ensures that individual participants are anonymized in the reported results, and that the model output was not publicly shared. The measurements from the meteorological masts FINO3, Høsøre, and Cabauw, are provided by the data owners under an agreement of not sharing the data with any 3rd party.

Competing interests. The authors declare that they have no conflict of interests

Acknowledgements. Funding from the EU and the Danish Energy Agency through the project EUDP 14-II, ERA-NET Plus - "New European Wind Atlas" is greatly appreciated. The authors would also like to thank the European Wind Energy Association (EWEA) for organizing this mesoscale benchmarking study, the German Federal Ministry for the Environment, Nature Conservation and Nuclear Safety (BMU), and the Project Management Jülich (PTJ) for sharing the FINO3 mast data, and the Cabauw Experimental Site for Atmospheric Research (CESAR) for making the measurements from the Cabauw mast freely available online (www.cesar-labaratory.nl). Furthermore, we would like to thank the Test and Measurement section of DTU for providing the Høvsøre mast data, and finally we would like to thank the participants for providing their model data for the intercomparison.

Wind Energ. Sci. Discuss., doi:10.5194/wes-2016-43, 2016
Manuscript under review for journal Wind Energ. Sci.
Published: 1 December 2016

eawe european academy of wind energy
Open Access WIND ENERGY SCIENCE DISCUSSIONS

References

Al-Yahyai, S., Charabi, Y., Al-Badi, A., and Gastli, A.: Nested ensemble NWP approach for wind energy assessment, Renewable Energy, 37, 150–160, doi:10.1016/j.renene.2011.06.014, http://dx.doi.org/10.1016/j.renene.2011.06.014, 2012.

Arino, O., Bicheron, P., Achard, F., and Latham, J.: The most detailed portrait of Earth, Eur. Space Agency, http://www.esa.int/esapub/bulletin/bulletin136/bul136d_arino.pdf, 2008.

Badger, J., Frank, H., Hahmann, A. N., and Giebel, G.: Wind-Climate Estimation Based on Mesoscale and Microscale Modeling: Statistical–Dynamical Downscaling for Wind Energy Applications, Journal of Applied Meteorology and Climatology, 53, 1901–1919, doi:10.1175/JAMC-D-13-0147.1, http://journals.ametsoc.org/doi/abs/10.1175/JAMC-D-13-0147.1, 2014.

Bechmann, A., Sørensen, N. N., Berg, J., Mann, J., and Réthoré, P. E.: The Bolund Experiment, Part II: Blind Comparison of Microscale Flow Models, Boundary-Layer Meteorology, 141, 245–271, doi:10.1007/s10546-011-9637-x, 2011.

Berg, J., Mann, J., Bechmann, A., Courtney, M. S., and Jørgensen, H. E.: The Bolund Experiment, Part I: Flow Over a Steep, Three-Dimensional Hill, Boundary-Layer Meteorology, 141, 219–243, doi:10.1007/s10546-011-9636-y, 2011.

Bowler, N. E., Pierce, C. E., and Seed, A. W.: STEPS: A probabilistic precipitation forecasting scheme which merges an extrapolation nowcast with downscaled NWP, Quarterly Journal of the Royal Meteorological Society, 132, 2127–2155, doi:10.1256/qj.04.100, http://doi.wiley.com/10.1256/qj.04.100, 2006.

Büttner, G., Feranec, J., and Jaffrain, G.: The CORINE land cover 2000 project, EARSeL . . . , http://www.eproceedings.org/static/vol03_3/03_3_buttner2.pdf, 2004.

Carvalho, D., Rocha, A., Gómez-Gesteira, M., and Santos, C.: A sensitivity study of the WRF model in wind simulation for an area of high wind energy, Environmental Modelling & Software, 33, 23–34, doi:10.1016/j.envsoft.2012.01.019, http://linkinghub.elsevier.com/retrieve/pii/S1364815212000382, 2012.

Carvalho, D., Rocha, a., Gómez-Gesteira, M., and Silva Santos, C.: WRF wind simulation and wind energy production estimates forced by different reanalyses: Comparison with observed data for Portugal, Applied Energy, 117, 116–126, doi:10.1016/j.apenergy.2013.12.001, http://dx.doi.org/10.1016/j.apenergy.2013.12.001, 2014a.

Carvalho, D., Rocha, a., Gómez-Gesteira, M., and Silva Santos, C.: Sensitivity of the WRF model wind simulation and wind energy production estimates to planetary boundary layer parameterizations for onshore and offshore areas in the Iberian Peninsula, Applied Energy, 135, 234–246, doi:10.1016/j.apenergy.2014.08.082, http://linkinghub.elsevier.com/retrieve/pii/S0306261914008939, 2014b.

Champeaux, J. L., Masson, V., and Chauvin, F.: ECOCLIMAP: a global database of land surface parameters at I km resolution, Meteorological Applications, 12, 29–32, doi:10.1017/S1350482705001519, http://doi.wiley.com/10.1017/S1350482705001519, 2005.

Constantinescu, E. M., Zavala, V. M., Rocklin, M., Lee, S., and Anitescu, M.: A computational framework for uncertainty quantification and stochastic optimization in unit commitment with wind power generation, IEEE Transactions on Power Systems, 26, 431–441, doi:10.1109/TPWRS.2010.2048133, 2011.

Courtier, P., Thepaut, J. N., and Hollingsworth, a.: A Strategy for Operational Implementation of 4d-Var, Using an Incremental Approach, Quarterly Journal of the Royal Meteorological Society, 120, 1367–1387, doi:10.1002/qj.49712051912, 1994.

Cox, P. M., Betts, R. A., Bunton, C. B., Essery, R. L. H., Rowntree, P. R., and Smith, J.: The impact of new land surface physics on the GCM simulation of climate and climate sensitivity, Climate Dynamics, 15, 183–203, doi:10.1007/s003820050276, 1999.

Cuxart, J.: A turbulence scheme allowing for mesoscale and large-eddy simulations, Quarterly Journal of the Royal Meteorological Society, http://onlinelibrary.wiley.com/doi/10.1002/qj.49712656202/full, 2000.

Wind Energ. Sci. Discuss., doi:10.5194/wes-2016-43, 2016
Manuscript under review for journal Wind Energ. Sci.
Published: 1 December 2016

Dee, D. P., Uppala, S. M., Simmons, A. J., Berrisford, P., Poli, P., Kobayashi, S., Andrae, U., Balmaseda, M. A., Balsamo, G., Bauer, P., Bechtold, P., Beljaars, A. C. M., van de Berg, L., Bidlot, J., Bormann, N., Delsol, C., Dragani, R., Fuentes, M., Geer, A. J., Haimberger, L., Healy, S. B., Hersbach, H., Hólm, E. V., Isaksen, L., Kållberg, P., Köhler, M., Matricardi, M., Mcnally, A. P., Monge-Sanz, B. M., Morcrette, J. J., Park, B. K., Peubey, C., de Rosnay, P., Tavolato, C., Thépaut, J. N., and Vitart, F.: The ERA-Interim reanalysis: Configuration and performance of the data assimilation system, Quarterly Journal of the Royal Meteorological Society, 137, 553–597, doi:10.1002/qj.828, 2011.

Draxl, C., Hahmann, A. N., Peña, A., and Giebel, G.: Evaluating winds and vertical wind shear from Weather Research and Forecasting model forecasts using seven planetary boundary layer schemes, Wind Energy, 17, 39–55, doi:10.1002/we, http://onlinelibrary.wiley.com/doi/10.1002/we.1608/full, 2014.

Fabre, S., Stickland, M., Scanlon, T., and Oldroyd, A.: Measurement and simulation of the flow field around the FINO 3 triangular lattice meteorological mast, Journal of Wind, http://www.sciencedirect.com/science/article/pii/S0167610514000804, 2014.

Friedl, M. A., Sulla-Menashe, D., Tan, B., Schneider, A., Ramankutty, N., Sibley, A., and Huang, X.: MODIS Collection 5 global land cover: Algorithm refinements and characterization of new datasets, Remote Sensing of Environment, 114, 168–182, doi:10.1016/j.rse.2009.08.016, http://dx.doi.org/10.1016/j.rse.2009.08.016, 2010.

Garbarino, R., Struzeski, T., and Casadevall, T.: US Geological Survey, http://citeseerx.ist.psu.edu/viewdoc/summary?doi=10.1.1.404.5834, 2002.

García-Díez, M., Fernández, J., Fita, L., and Yagüe, C.: Seasonal dependence of WRF model biases and sensitivity to PBL schemes over Europe, Quarterly Journal of the Royal Meteorological Society, 139, 501–514, doi:10.1002/qj.1976, 2013.

Gebhardt, C., Theis, S., Paulat, M., and Ben Bouallègue, Z.: Uncertainties in COSMO-DE precipitation forecasts introduced by model perturbations and variation of lateral boundaries, Atmospheric Research, 100, 168–177, doi:10.1016/j.atmosres.2010.12.008, 2011.

Gómez-Navarro, J. J., Raible, C. C., and Dierer, S.: Sensitivity of the WRF model to PBL parametrisations and nesting techniques: Evaluation of wind storms over complex terrain, Geoscientific Model Development, 8, 3349–3363, doi:10.5194/gmd-8-3349-2015, 2015.

Grell, G., Dudhia, J., and Stauffer, D.: A description of the fifth-generation Penn State/NCAR mesoscale model (MM5), https://www.researchgate.net/profile/Georg_Grell/publication/230642695_A_description_of_the_fifth-generation_Penn_StateNCAR_Mesoscale_Model_MM5/links/00b7d51b624259ae9f000000.pdf, 1994.

Hahmann, A. N., Badger, J., Vincent, C. L., Kelly, M. C., Volker, P. J. H., and Refslund, J.: Mesoscale modeling for the wind atlas for South Africa (WASA) Project, Tech. rep., DTU Wind Energy, 2014a.

Hahmann, A. N., Vincent, C. L., Peña, A., Lange, J., and Hasager, C. B.: Wind climate estimation using WRF model output: method and model sensitivities over the sea, International Journal of Climatology, doi:10.1002/joc.4217, http://doi.wiley.com/10.1002/joc.4217, 2014b.

Hahmann, A. N., Lennard, C., Badger, J., Vincent, C. L., Kelly, M. C., Volker, P. J. H., and Refslund, J.: Mesoscale modeling for the Wind Atlas of South Africa (WASA) project, DTU Wind Energy, No. 0050, 80 pp, doi:10.13140/RG.2.1.3735.6887, 2015.

Hong, S.-Y., Noh, Y., and Dudhia, J.: A New Vertical Diffusion Package with an Explicit Treatment of Entrainment Processes, Monthly Weather Review, 134, 2318–2341, doi:10.1175/MWR3199.1, http://journals.ametsoc.org/doi/abs/10.1175/MWR3199.1?prevSearch=&searchHistoryKey=, 2006.

Horvath, K., Koracin, D., Vellore, R., Jiang, J., and Belu, R.: Sub-kilometer dynamical downscaling of near-surface winds in complex terrain using WRF and MM5 mesoscale models, Journal of Geophysical Research Atmospheres, 117, 1–19, doi:10.1029/2012JD017432, 2012.

Wind Energ. Sci. Discuss., doi:10.5194/wes-2016-43, 2016
Manuscript under review for journal Wind Energ. Sci.
Published: 1 December 2016

Jackson, P. S. and Hunt, J. C. R.: Turbulent wind flow over a low hill, Quarterly Journal of the Royal Meteorological Society, 101, 929–955, doi:10.1002/qj.49710143015, http://doi.wiley.com/10.1002/qj.49710143015%5Cnhttp://www.cpom.org/people/jcrh/QJRMS-101.pdf, 1975.

Janjić, Z.: Nonsingular implementation of the Mellor–Yamada level 2.5 scheme in the NCEP Meso model, NCEP office note, http://www.lib.ncep.noaa.gov/ncepofficenotes/files/on437.pdf, 2002.

Janjić, Z. I.: The Step-Mountain Eta Coordinate Model: Further Developments of the Convection, Viscous Sublayer, and Turbulence Closure Schemes, Monthly Weather Review, 122, 927–945, doi:10.1175/1520-0493(1994)122<0927:TSMECM>2.0.CO;2, http://journals.ametsoc.org/doi/abs/10.1175/1520-0493(1994)122%3C0927:TSMECM%3E2.0.CO;2?prevSearch=&searchHistoryKey=, 1994.

Kallberg, P.: The HIRLAM level 1 system, Documentation manual, https://scholar.google.dk/scholar?hl=en&q=the+hirlam+level+1+system&btnG=&as_sdt=1%252C5&as_sdtp=#0, 1989.

Kallos, G., Nickovic, S., and Papadopoulos, A.: The regional weather forecasting system SKIRON: An overview, Proceedings of the symposium on regional weather prediction on parallel computer environments, https://scholar.google.dk/scholar?hl=en&q=The+Regional+weather+forecasting+system+SKIRON&btnG=&as_sdt=1%252C5&as_sdtp=#0, 1997.

Kanamitsu, M., Ebisuzaki, W., Woollen, J., Yang, S. K., Hnilo, J. J., Fiorino, M., and Potter, G. L.: NCEP-DOE AMIP-II reanalysis (R-2), Bulletin of the American Meteorological Society, 83, 1631–1643+1559, doi:10.1175/BAMS-83-11-1631, 2002.

Lean, H. and Clark, P.: Characteristics of high-resolution versions of the Met Office Unified Model for forecasting convection over the United Kingdom, Monthly Weather Review, http://journals.ametsoc.org/doi/abs/10.1175/2008MWR2332.1, 2008.

Lock, a. P., Brown, a. R., Bush, M. R., Martin, G. M., and Smith, R. N. B.: A New Boundary Layer Mixing Scheme. Part I: Scheme Description and Single-Column Model Tests, Monthly Weather Review, 128, 3187–3199, doi:10.1175/1520-0493(2000)128<3187:ANBLMS>2.0.CO;2, http://journals.ametsoc.org/doi/abs/10.1175/1520-0493(2000)128%3C3187:ANBLMS%3E2.0.CO;2, 2000.

Loveland, T. R. and Belward, a. S.: The IGBP-DIS global 1km land cover data set, DISCover: First results, International Journal of Remote Sensing, 18, 3289–3295, doi:10.1080/014311697217099, 1997.

Mehrens, A. R., Hahmann, A. N., Larsén, X. G., and von Bremen, L.: Correlation and coherence of mesoscale wind speeds over the sea, Quarterly Journal of the Royal Meteorological Society, doi:10.1002/qj.2900, http://doi.wiley.com/10.1002/qj.2900, 2016.

Moigne, P. L. and Boone, A.: SURFEX scientific documentation, http://geosci-model-dev.net/6/929/2013/gmd-6-929-2013-supplement.pdf, 2009.

Mortensen, N. G., Nielsen, M., and Jørgensen, H. E.: Comparison of Resource and Energy Yield Assessment Procedures 2011-2015 : What have we learned and what needs to be done ? 1 Introduction 2 Case study wind farms, pp. 1–10, 2015.

Nakanishi, M. and Niino, H.: An Improved Mellor-Yamada Level-3 Model: Its Numerical Stability and Application to a Regional Prediction of Advection Fog, Boundary-Layer Meteorology, 119, 397–407, doi:10.1007/s10546-005-9030-8, http://www.springerlink.com/content/j04441r721280776/, 2006.

Niu, G.-Y., Yang, Z.-L., Mitchell, K. E., Chen, F., Ek, M. B., Barlage, M., Kumar, A., Manning, K., Niyogi, D., Rosero, E., Tewari, M., and Xia, Y.: The community Noah land surface model with multiparameterization options (Noah-MP): 1. Model description and evaluation with local-scale measurements, Journal of Geophysical Research, 116, D12 109, doi:10.1029/2010JD015139, http://doi.wiley.com/10.1029/2010JD015139, 2011.

Noilhan, J. and Mahfouf, J. F.: The ISBA land surface parameterisation scheme, Global and Planetary Change, 13, 145–159, doi:10.1016/0921-8181(95)00043-7, 1996.

Wind Energ. Sci. Discuss., doi:10.5194/wes-2016-43, 2016
Manuscript under review for journal Wind Energ. Sci.
Published: 1 December 2016

Orlanski, I.: A rational subdivision of scales for atmospheric processes, Bulletin of the American Meteorological Society, http://www.citeulike.org/group/17501/article/12086670, 1975.

Palmer, T. N., Alessandri, A., Andersen, U., Cantelaube, P., Davey, M., Délécluse, P., Déqué, M., Díez, E., Doblas-Reyes, F. J., Feddersen, H., Graham, R., Gualdi, S., Guérémy, J. F., Hagedorn, R., Hoshen, M., Keenlyside, N., Latif, M., Lazar, A., Maisonnave, E., Marletto, V., Morse, A. P., Orfila, B., Rogel, P., Terres, J. M., and Thomson, M. C.: Development of a European multimodel ensemble system for seasonal-to-interannual prediction (DEMETER), Bulletin of the American Meteorological Society, 85, 853–872, doi:10.1175/BAMS-85-6-853, 2004.

Pan, H. L. and Mahrt, L.: Interaction between soil hydrology and boundary-layer development, Boundary-Layer Meteorology, 38, 185–202, doi:10.1007/BF00121563, 1987.

Peña, A., Floors, R., and Gryning, S. E.: The Høvsøre Tall Wind-Profile Experiment: A Description of Wind Profile Observations in the Atmospheric Boundary Layer, Boundary-Layer Meteorology, 150, 69–89, doi:10.1007/s10546-013-9856-4, 2014.

Pielke, R., Cotton, W., and Walko, R.: A comprehensive meteorological modeling system—RAMS, Meteorology and Atmospheric Physics, http://link.springer.com/article/10.1007/BF01025401, 1992.

Pleim, J.: A Simple, Efficient Solution of Flux–Profile Relationships in the Atmospheric Surface Layer, Journal of Applied Meteorology and Climatology, 45, 341–347, doi:10.1175/JAM2339.1, http://ams.allenpress.com/perlserv/?request=get-abstract&doi=10.1175/JAM2339.1%5Cnpapers2://publication/doi/10.1175/JAM2339.1, 2006.

Pleim, J. E.: A combined local and nonlocal closure model for the atmospheric boundary layer. Part I: Model description and testing, Journal of Applied Meteorology and Climatology, 46, 1383–1395, doi:10.1175/JAM2539.1, 2007a.

Pleim, J. E.: A Combined Local and Nonlocal Closure Model for the Atmospheric Boundary Layer. Part II: Application and Evaluation in a Mesoscale Meteorological Model, Journal of Applied Meteorology and Climatology, 46, 1396–1409, doi:10.1175/JAM2534.1, http://journals.ametsoc.org/doi/abs/10.1175/JAM2534.1, 2007b.

Rienecker, M. M., Suarez, M. J., Gelaro, R., Todling, R., Bacmeister, J., Liu, E., Bosilovich, M. G., Schubert, S. D., Takacs, L., Kim, G. K., Bloom, S., Chen, J., Collins, D., Conaty, A., Da Silva, A., Gu, W., Joiner, J., Koster, R. D., Lucchesi, R., Molod, A., Owens, T., Pawson, S., Pegion, P., Redder, C. R., Reichle, R., Robertson, F. R., Ruddick, A. G., Sienkiewicz, M., and Woollen, J.: MERRA: NASA's modern-era retrospective analysis for research and applications, Journal of Climate, 24, 3624–3648, doi:10.1175/JCLI-D-11-00015.1, 2011.

Saha, S., Moorthi, S., Pan, H. L., Wu, X., Wang, J., Nadiga, S., Tripp, P., Kistler, R., Woollen, J., Behringer, D., Liu, H., Stokes, D., Grumbine, R., Gayno, G., Wang, J., Hou, Y. T., Chuang, H. Y., Juang, H. M. H., Sela, J., Iredell, M., Treadon, R., Kleist, D., Van Delst, P., Keyser, D., Derber, J., Ek, M., Meng, J., Wei, H., Yang, R., Lord, S., Van Den Dool, H., Kumar, A., Wang, W., Long, C., Chelliah, M., Xue, Y., Huang, B., Schemm, J. K., Ebisuzaki, W., Lin, R., Xie, P., Chen, M., Zhou, S., Higgins, W., Zou, C. Z., Liu, Q., Chen, Y., Han, Y., Cucurull, L., Reynolds, R. W., Rutledge, G., and Goldberg, M.: The NCEP climate forecast system reanalysis, Bulletin of the American Meteorological Society, 91, 1015–1057, doi:10.1175/2010BAMS3001.1, 2010.

Schicker, I., Arnold Arias, D., and Seibert, P.: Influences of updated land-use datasets on WRF simulations for two Austrian regions, Meteorology and Atmospheric Physics, 128, 279–301, doi:10.1007/s00703-015-0416-y, http://link.springer.com/10.1007/s00703-015-0416-y, 2016.

Seity, Y., Brousseau, P., Malardel, S., Hello, G., Bénard, P., Bouttier, F., Lac, C., and Masson, V.: The AROME-France Convective-Scale Operational Model, Monthly Weather Review, 139, 976–991, doi:10.1175/2010MWR3425.1, 2011.

Simmons, A., Uppala, S., Dee, D., and Kobayashi, S.: ERA-Interim: New ECMWF reanalysis products from 1989 onwards, ECMWF newsletter, 110(110), 25–35., 2007.

Wind Energ. Sci. Discuss., doi:10.5194/wes-2016-43, 2016
Manuscript under review for journal Wind Energ. Sci.
Published: 1 December 2016

Skamarock, W. C., Klemp, J. B., Dudhia, J., Gill, D. O., Barker, D. M., Duda, M. G., Huang, X.-Y., Wang, W., and Powers, J. G.: A Description of the Advanced Research WRF Version 3, 2008a.

Skamarock, W. C., Klemp, J. B., Dudhia, J., Gill, D. O., Barker, D. M., Duda, M. G., Huang, X.-Y., Wang, W., and Powers, J. G.: A Description of the Advanced Research WRF Version 3, 2008b.

Storm, B., Dudhia, J., Basu, S., Swift, A., and Giammanco, I.: Evaluation of the weather research and forecasting model on forecasting low-level jets: Implications for wind energy, Wind Energy, 12, 81–90, doi:10.1002/we.288, 2009.

Sukoriansky, S., Galperin, B., and Perov, V.: Application of a New Spectral Theory of Stably Stratified Turbulence to the Atmospheric Boundary Layer over Sea Ice, Boundary-Layer Meteorology, 117, 231–257, doi:10.1007/s10546-004-6848-4, http://link.springer.com/10.1007/s10546-004-6848-4, 2005.

Ulden, A. V. and Wieringa, J.: Atmospheric boundary layer research at Cabauw, Boundary-Layer Meteorology 25th Anniversary, http://link.springer.com/chapter/10.1007/978-94-017-0944-6{_}3, 1996.

Vincent, C. L. and Hahmann, A. N.: The impact of grid and spectral nudging on the variance of the near-surface wind speed, Journal of Applied Meteorology and Climatology, 54, 1021–1038, doi:10.1175/JAMC-D-14-0047.1, 2015.

Walko, R. and Tremback, C.: ATMET Technical Note 1, Modifications for the Transition from LEAF-2 to LEAF-3, ATMET, LLC, Boulder, Colorado 80308-2195, https://scholar.google.dk/scholar?hl=en&q=ATMET+Technical+Note+1%252C+Modifications+for+the+Transition+from+LEAF-2+to+LEAF-3%252C+AT&btnG=&as_sdt=1%252C5&as_sdtp=#0, 2005.

Warner, T. T.: Numerical Weather and Climate Prediction, 2004.

Wind Energ. Sci. Discuss., doi:10.5194/wes-2016-43, 2016
Manuscript under review for journal Wind Energ. Sci.
Published: 1 December 2016

eawe european academy of wind energy
Open Access WIND ENERGY SCIENCE DISCUSSIONS

Table A1. Site description, including latitude and longitude coordinates, classification of the site, and the height of the mast z_s as well as the location terrain elevation relative to sea-level z_{asl} and prevailing wind direction.

Nr.	Name	Latitude [°]	Longitude [°]	Type	z_s [m]	z_{asl} [m]	Prev. wind direction
1	FINO3	55.195	7.158	Offshore	120	0	WSW
2	Høvsøre	56.441	8.151	Coastal	116	2	WSW
3	Cabuaw	51.970	4.926	Inland	213	-1	SW
4	Dataless1	57.673	9.024	Offshore	-	0	WSW
5	Dataless2	56.011	10.354	Coastal	-	0	SE
6	Dataless3	52.830	10.000	Inland	-	77	SE

Wind Energ. Sci. Discuss., doi:10.5194/wes-2016-43, 2016
Manuscript under review for journal Wind Energ. Sci.
Published: 1 December 2016

eawe european academy of wind energy
Open Access WIND ENERGY SCIENCE DISCUSSIONS

Table A2. Intercomparison heights for each site (marked by the x).

Height $[m]$	FINO3	Høvsøre	Cabauw	Dataless1-3
200			x	
140			x	
120				x
100		x		x
90	x			
80		x	x	x
60	x	x		
40	x	x	x	x
20			x	x
10	x	x	x	x

Wind Energ. Sci. Discuss., doi:10.5194/wes-2016-43, 2016
Manuscript under review for journal Wind Energ. Sci.
Published: 1 December 2016

eawe european academy of wind energy
Open Access WIND ENERGY SCIENCE DISCUSSIONS

Table A3. Variables submitted by contributers.

Variable name	Symbol	Units
Bulk Richardson number	R_i	
(Obukov length)$^{-1}$	$1/L$	m^{-1}
Surface temperature	T_s	K
Air temperature	T	K
Wind speed	u	m/s
Wind direction		$^\circ$
Specific humidity	Q	kg/kg

Wind Energ. Sci. Discuss., doi:10.5194/wes-2016-43, 2016
Manuscript under review for journal Wind Energ. Sci.
Published: 1 December 2016

eawe european academy of wind energy
Open Access WIND ENERGY SCIENCE DISCUSSIONS

Table A4. Participants in the study in alphabetical order.

Participant	Institution	Country
3E	Company	Belgium
Anemos GmbH	Company	Germany
ATM Pro	Company	Belgium
CENER	Research Center	Spain
CIEMAT	Research Center	Spain
DEWI	Company	Germany
DTU Wind Energy	University	Denmark
DX Wind Technologies	Company	China
EMD International	Company	Denmark
ISAC-CNR	Research Center	Italy
KNMI	Meteorological institute	The Netherlands
Met Office	Meteorological institute	United Kingdom
RES ltd.	Company	United Kingdom
Statiol ASA	Company	Norway
University of Oldenburg	University	Germany
Vestas	Company	Denmark
Vortex	Company	Spain

Wind Energ. Sci. Discuss., doi:10.5194/wes-2016-43, 2016
Manuscript under review for journal Wind Energ. Sci.
Published: 1 December 2016

eawe european academy of wind energy
Open Access WIND ENERGY SCIENCE DISCUSSIONS

Table A5. Setup description of the 25 model setups ranked by horizontal grid spacing of the finest grid. The columns are: the model name and version (Model), the PBL scheme (PBL), the land surface model (LSM), whether nesting was used (Nest.), the horizontal grid spacing (Δ), the land cover source, Simulation and spinup time (Sim. time), and initial and boundary condition data (B.C.).

Nr.	Model	PBL	LSM	Nest.	Δ [km]	Landcover	Sim. time [h]	B.C.
1	WRF V3.6.1[a]	Custom	-	yes	1	CORINE[b]	48-24	Era-I[c]
2	MAESTRO V15.01	-	-	no	1	CORINE	-	Era-I
3	WRF V3.6.1	MYJ[d]	Noah[e]	yes	2	USGS[f]	78-6	Era-I
4	WRF V3.3.1	MYJ	-	yes	2	GlobCover[g]	11064-24	Era-I
5	WRF V3.5.1	YSU[h]	Noah	yes	2	CORINE	30-6	Era-I
6	WRF V3.5.1	YSU	Noah	yes	2	-	264-24	Era-I
7	HARMONIE V37h1.1[i]	SURFEX[j]	ISBA[k]	yes	1.5	ECOCLIMAP[l]	7-1	Era-I
8	WRF V3.6	ACM2[m]	Noah	yes	3	USGS-MODIS	84-12	FNL[n]
9	WRF V3.4	MYJ	Noah	no	3	USGS	28-4	Era-I
10	WRF V3.6.1	YSU	Noah	yes	3	CORINE	672-96	CFSR[o]
11	WRF V3.0.1	MYJ	Noah	yes	3	GlobCover	36-6	CFSR
12	WRF V3.6.1	MYNN[p]	Noah	yes	3	USGS	816-72	Era-I
13	WRF V3.0.1	MYJ	Noah	yes	3	GlobCover	36-12	MERRA[q]
14	WRF V3.0.1	MYJ	Noah	yes	3	GlobCover	36-12	Era-I
15	WRF V3.1	MYJ	Noah	yes	3	MODIS[r]	54-6	FNL
16	WRF V3.6.1	YSU	Noah	yes	3	CORINE	336-96	CFSR
17	WRF V3.5.1	MYJ	Noah	yes	4	IGBP-MODIS[s]	264-24	Era-I
18	UM V8.4[t]	Lock[u]	JULES[v]	yes	4	IGBP-MODIS	36-6	Era-I
19	WRF V3.5.1	YSU	Noah	yes	5	USGS	8856-24	Era-I
20	SKIRON V6.9[w]	MYNN	OSU[x]	no	5	USGS	51-3	GFS[y]
21	WRF V3.5.1	YSU	Noah	yes	5	USGS	8856-24	Era-I
22	WRF V3.5.1	YSU	Noah	yes	6	IGBP-MODIS	264-24	Era-I
23	HIRLAM V6.4.2[z]	CBR[aa]	ISBA	no	11	USGS	9-3	IFS[ab]
24	RAMS V6.0[ac]	MYNN	LEAF[ad]	no	12	CORINE	36-12	IFS
25	MM5 V3[ae]	YSU	-	no	20	CORINE	744-24	MERRA

[a] Skamarock et al. (2008b)
[b] Büttner et al. (2004)
[c] Dee et al. (2011)
[d] Janjić (2002)
[e] Niu et al. (2011)
[f] Garbarino et al. (2002)
[g] Arino et al. (2008)
[h] Hong et al. (2006)
[i] Seity et al. (2011)
[j] Moigne and Boone (2009)
[k] Noilhan and Mahfouf (1996)
[l] Champeaux et al. (2005)
[m] Pleim (2007a)
[n] NCEP Final analysis
[o] Saha et al. (2010)
[p] Nakanishi and Niino (2006)
[q] Rienecker et al. (2011)
[r] Friedl et al. (2010)
[s] Loveland and Belward (1997)
[t] Lean and Clark (2008)
[u] Lock et al. (2000)
[v] Cox et al. (1999)
[w] Kallos et al. (1997)
[x] Pan and Mahrt (1987)
[y] Global Forecast System
[z] Kallberg (1989)
[aa] Cuxart (2000)
[ab] Integrated Forecasting System
[ac] Pielke et al. (1992)
[ad] Walko and Tremback (2005)
[ae] Grell et al. (1994)